People's Democratic Republic of Algeria
University Kasdi Merbah of Ouargla
Faculty of New Information and Communication Technologies
Department of Electronics and Telecommunications

Academic Master's thesis

To obtain the degree of master delivered by Specialty:

TELECOMMUNICATIONS SYSTEMS

Direction of arrival estimation methods for coherent and non-coherent sources

Presented publicly

BEKHTA ISRA
KINA MARIA

Before the jury composed of:

Mr MOAD Mohamed Sayah	M.C.A	President	UKM Ouargla
Mr CHENINA Hachemi	M.C.B	Examiner	UKM Ouargla
Mr AOUNALLAH Naceur	Professor	Supervisor	UKM Ouargla

Academic Year: 2024 / 2025

Dedication

For every beginning, there is an end, and for every end, there is an arrival. The journey hasn't been short, nor should it be. The dream was not close, nor was the road fraught with facilities, but I did it with God's help. Praise be to God with love and gratitude, thanks to whom I am today crowned with a long-awaited dream that has become a reality that I am proud of. To those who, thanks to them, I am here today, my constant supporters after God, my beloved parents, without whom this achievement would not have existed, all thanks and gratitude for what you gave me. To those who said, We will strengthen you with your brothers, thank you for your support. To my friends on the path, thank you for your support.

ISRA

إهداء

سورة يوسف - آية 76

﴿ وَفَوْقَ كُلِّ ذِي عِلْمٍ عَلِيمٌ ﴾

الحمد لله أولاً وآخراً، وبفضله يتحقق الإنجاز، وبنوره نهتدي في طريق العلم والمعرفة.
له الحمد كما ينبغي لجلال وجهه وعظيم سلطانه، على ما وهبني من نعمة العقل، وصحة الجسد، وحسن الخلق، وما يسر لي من سُبل الوصول إلى هذه اللحظة.

إلى من غادرت هذا العالم ولكنها لم تغادر قلبي، إلى جدتي الحبيبة (رحمها الله)، التي أهدتني من حبها وحنانها ما يكفيني عمراً بأكمله... رحمكِ الله وأسكنكِ فسيح جناته.
إلى والديَّ الكريمين، منبع الحب والدعم، وكل الامتنان لا يكفي لقلبيكما.
إلى إخوتي الأعزاء، أدعو الله أن يوفقكم في حياتكم، وأن يسعد قلوبكم كما أسعدتم قلبي دائمًا.
إلى رفيق دربي، شكرًا لوجودك بجانبي، لثباتك حين تعبت، وابتسامتك حين احتجت، كنتَ العون والدافع في كل خطوة.
إلى عائلتي الكبيرة، التي أعتز بانتمائي إليها، وبكل فردٍ فيها كان له أثر.
إلى أصدقائي وصديقاتي، أنتم النور الذي رافقني في الدرب، والضحكة التي خففت عني التعب، شكرًا لكل لحظة صادقة بيننا.
إلى ذاتي، أهديكِ هذا الإنجاز بعد رحلةٍ من الصعوبات، فكنتِ قوية، صبورة، مؤمنة... فاستحققتِ النجاح.
وأخص بالشكر والتقدير:

- معلمتي في المرحلة الابتدائية: **خراز آسياء**، التي غرست فيّ حبّ التعلم منذ الخطوة الأولى.
- أستاذة الرياضيات في الطور المتوسط: **كل صليحة**، التي جعلتني أرى الجمال في المنطق.
- أستاذة الرياضيات في الطور الثانوي: **بدو ربيعة**، التي آمنت بقدراتي قبل أن أفعل أنا.
- أستاذ اللغة الإنجليزية: **بن شعبان مهدي**، الذي علّمني الصبر وطول البال، فكان له الأثر الكبير في تطوير مهاراتي.

لكم جميعًا، خالص الامتنان من قلب لا ينسى من كان له في مسيرتي أثر.

مارية

Acknowledgment

Alhamdulillah for completion and perfection. First of all, we extend our sincere thanks and gratitude to our supervisor Prof. AOUNALLAH Naceur for his help, valuable supervision, and advice in completing this work. We thank everyone who taught us a letter in our educational journey. We thank our families for their constant support in this educational journey.

Thanks to everyone...

Abstract

In light of the swift advancement of wireless communication technologies, smart antenna systems have become essential tools for enhancing signal transmission and reception. These systems combine multiple antenna elements with sophisticated signal processing algorithms, including beamforming and Direction of Arrival (DoA) estimation, allowing them to adapt dynamically to their surroundings. Important DoA estimation methods such as MUSIC, ESPRIT, and Min-Norm are assessed, along with improvement techniques like spatial smoothing and Toeplitz matrix reconstruction, which tackle issues related to signal coherence. The introduced algorithms—AT-MUSIC and AT-MN—exhibit enhanced accuracy and resilience in intricate situations. As the need for increased data rates and resistance to interference escalates, especially with the progress of networks, smart antenna systems remain a promising avenue for solutions. Future research may investigate machine learning techniques and real-time applications to further boost system efficacy.

Keywords: Smart Antenna Systems; Direction of Arrival (DoA); Beamforming; MUSIC; ESPRIT; Min-Norm; Spatial Smoothing; Toeplitz Matrix; AT-MUSIC; AT-MN ; Signal Processing.

Résumé

Étant donné les avancées rapides des technologies de communication sans fil, les systèmes d'antennes intelligentes sont devenus des outils indispensables pour optimiser la transmission et la réception des signaux. Ces systèmes intègrent plusieurs éléments d'antenne avec des algorithmes avancés de traitement du signal, tels que la formation de faisceaux et l'estimation de la direction d'arrivée, leur permettant de s'adapter de manière dynamique à leur environnement. Des méthodes significatives d'estimation de la direction d'arrivée, comme MUSIC, ESPRIT et Min-Norm, sont examinées, ainsi que des techniques d'amélioration telles que le lissage spatial et la reconstruction de la matrice de Toeplitz, qui traitent les problèmes de cohérence du signal. Les algorithmes proposés - AT-MUSIC et AT-MN - démontrent une précision et une robustesse accrues dans des contextes complexes. Alors que la demande pour des débits de données plus élevés et une meilleure résistance aux interférences croît, notamment avec l'évolution des réseaux , les systèmes d'antennes intelligentes demeurent une voie prometteuse pour développer des solutions. Les recherches à venir pourraient se concentrer sur les techniques d'apprentissage automatique et les applications en temps réel pour améliorer encore l'efficacité du système.

Mots clés: systèmes d'antennes intelligentes; formation de faisceaux; estimation de la direction d'arrivée; MUSIC; ESPRIT; Min-Norm; lissage spatial; matrice de Toeplitz; réseaux .

الملخص

نظراً للتقدم السريع في تقنيات الاتصال اللاسلكي، أصبحت أنظمة الهوائيات الذكية أدوات أساسية لتحسين نقل واستقبال الإشارات. تجمع هذه الأنظمة بين عدة عناصر هوائية مع خوارزميات متطورة لمعالجة الإشارة، بما في ذلك تشكيل الحزم وتقدير اتجاه الوصول، مما يتيح لها التكيف ديناميكيًا مع بيئتها. يتم تقييم طرق هامة لتقدير اتجاه الوصول، مثل MUSIC وESPRIT وMin-Norm، بالإضافة إلى تقنيات تحسين مثل التنعيم المكاني وإعادة بناء مصفوفة توبليز، التي تعالج المشكلات المتعلقة بتناسق الإشارة. تظهر الخوارزميات المقدمة - AT-MUSIC وAT-MN - دقة ومقاومة متزايدتين في الحالات المعقدة. مع تزايد الحاجة إلى سرعات بيانات أعلى ومقاومة للتداخل، خاصة مع تقدم شبكات ، تظل أنظمة الهوائيات الذكية مساراً واعداً لإيجاد الحلول. قد تركز الأبحاث المستقبلية على تقنيات التعلم الآلي والتطبيقات في الوقت الحقيقي لتحسين كفاءة النظام بشكل أكبر.

الكلمات المفتاحية: أنظمة الهوائيات الذكية؛ تشكيل الحزم؛ تقدير اتجاه الوصول؛ ؛MUSIC ؛Min-Norm ESPRIT ؛ التنعيم المكاني؛ مصفوفة توبليز؛ .

List of Symbols and Abbreviations

$(\cdot)^H$ Hermitian (conjugate transpose) operator

$(\cdot)^T$ Transpose operator

α Elevation angle

η The effeciency

$\hat{\rho}_{xy}(r\Delta t)$ Discrete approximation of the cross-correlation coefficient

$\hat{R}$ Estimated sample covariance matrix

$\hat{R}_{xx}(r\Delta t)$ Sample-based estimate of autocorrelation for discrete signal $x(n)$

$\hat{R}_{xy}(r\Delta t)$ Sample-based estimate of cross-correlation between $x(n)$ and $y(n)$

$\hat{R}_{yy}(r\Delta t)$ Sample-based estimate of autocorrelation for $y(t)$

ω Weight vector for the spatial filter

ω^H Hermitian (conjugate transpose) of the weight vector

$\rho_{xy}(\tau)$ Cross-correlation coefficient (normalized correlation)

$\rho^2_{xy}(f)$ Magnitude-squared coherence between signals x and y at frequency f

σ^2 Variance of Gaussian noise

θ The site angle

φ Azimuth angle

$\vec{E}$ The electric field

$a^H(\theta)$ Hermitian transpose (conjugate transpose) of the steering vector

$D(\theta, \phi)$ The directivity

$G(\theta, \phi)$ The Gain

$n(t)$ $M \times 1$ complex noise vector

$P(\theta, \phi)$ Power

P_A The input electrical power

P_R Radiated Power

$P_{\text{Capon}}(\theta)$ Capon spatial power spectrum function

$P_{\text{MIN\_NORM}}(\theta)$ Min-Norm spatial pseudo-spectrum function

$P_{\text{MUSIC}}(\theta)$ MUSIC spatial spectrum function

$P_{\text{PM}}(\theta)$ Spatial spectrum for the Propagator Method

R_{ii} Covariance matrix of the i^{th} forward-smoothed sub-array

R_{ss} Covariance matrix of the source signals

R_{xx} Covariance matrix of the received signal

$R_{xx}(\tau)$ Autocorrelation function of $x(t)$

R_{xx}^{-1} Inverse of the covariance matrix

$R_{xy}(\tau)$ Cross-correlation function between $x(t)$ and $y(t)$

$S(t)$ $K \times 1$ source signal vector at time t

$S_{xx}(f)$ Power spectral density of signal x

$S_{yy}(f)$ Power spectral density of signal y

V_N Matrix of eigenvectors spanning the noise subspace

V_s Matrix of eigenvectors spanning the signal subspace

$V_s^H x$ Orthogonality constraint (i.e., x is in the noise subspace)

x_n Snapshot of the received signal vector at time index n

x_n^H Hermitian (conjugate transpose) of x_n

AC Averaging Consensus

AoA Angle of Arrival

AT-MN Averaging Toeplitz for Min-Norm

CAPON Capon's Method (also known as MVDR)

CM Covariance Matrix

CVT Cross-Correlation Vectors Toeplitz

DoA Direction of Arrival

E[.] Expectation operator

ESPRIT Estimation of Signal Parameters via Rotational Invariance Techniques

EVD Eigenvalue Decomposition

LMS Least Mean Squares

MIN-NORM Minimum Norm Method

MUSIC Multiple Signal Classification

PC Coherent Processing

PM Propagation Method

R_S Signal covariance matrix

RMSE Root Mean Square Error

RN Noise covariance matrix

SIMO Single Input Multiple Output

SNR Signal-to-Noise Ratio

TOP Toeplitz Method

ULA Uniform Linear Array

List of Figures

Contents

General introduction

In light of the rapid advancements in wireless communication technologies, there has been an increasing need for smarter and more flexible antenna systems to enhance the efficiency of signal transmission and reception. Smart Antenna Systems represent a foundational pillar in this field, as they combine multiple antenna configurations with advanced signal processing algorithms to adapt to the surrounding environment and precisely steer signals toward their sources. These systems rely on several advanced engineering principles, most notably beamforming and Direction of Arrival (DoA) estimation, which allow the antenna to track signal sources and significantly improve the signal-to-noise ratio. Smart antennas come in various types and can generally be classified into fixed-beam antennas and adaptive antennas that rely on feedback mechanisms. The core architecture of adaptive antenna systems involves integrating a set of antenna elements with digital processors capable of analyzing signal characteristics and determining their angle of arrival. Among the most prominent algorithms used in DoA estimation are MUSIC and ESPRIT, along with spatial analysis methods such as the Min-Norm algorithm, which demonstrates high efficiency in environments with multiple signal sources. These systems face several challenges, particularly when dealing with correlated or coherent signals, which can degrade the performance of estimation algorithms. To address this issue, techniques such as Spatial Smoothing and the Toeplitz method have been developed, which reconstruct the covariance matrix in a way that mitigates the negative effects of signal correlation. Additionally, new algorithms have been proposed that enhance the mathematical structure of these matrices to achieve better performance under challenging operating conditions. Smart antenna systems and their wide range of applications are increasingly prominent in modern communication networks, such as 5G networks and advanced satellite communication systems, where they play a vital role in improving coverage, reducing interference, and achieving high spectral efficiency. These systems currently constitute one of the most active areas of scientific and engineering research, due to their potential to offer effective and sustainable solutions to the complex challenges of modern wireless communication. In this report

- **Chapter 1** provided foundational definitions of antenna arrays and smart antenna systems, along with their key functions, advantages of adaptive antennas, practical applications, and an overview of angle of arrival estimation.

- **Chapter 2** focused on DoA estimation techniques, including methods used to overcome issues of signal correlation and coherency.
- **Chapter 3** presented the simulation results and offered a discussion of the outcomes.

Chapter I

Antenna arrays

I.1 Introduction

Many refer to smart antenna systems as smart antennas, but in reality antennas by themselves are not smart. It is the digital signal processing capability, along with the antennas, which make the system smart. Although it may seem that smart antenna systems are a new technology, the fundamental principles upon which they are based are not new.
In this chapter defines antenna arrays, focusing on their types, functionality, and applications. It also delves into adaptive antenna systems, explaining how they function and their potential advantages. The concept of Direction of Arrival (DoA) estimation and beamforming techniques will also be discussed, demonstrating their relevance in improving the efficiency and effectiveness of modern communication systems. The aim of this chapter is to provide a comprehensive understanding of the theory and practical applications of antenna arrays, particularly in the context of adaptive antenna systems.

I.2 Antennas and their specifications

I.2.1 Definition

An antenna is a device that ensures the transition, or inversely, between an wave guide and the free space in which these wave will propagate. Antennas can be used to send or receive signals at various frequencies. In addition, some antennas can operate both in the emission and in the reception fields. There are various antenna types (Figure I.1 shows some examples), each possessing unique features. Their shape is often the most distinguishing characteristic. Antennas come in a vast array of shapes and sizes, designed for different frequencies, applications, and radiation patterns.

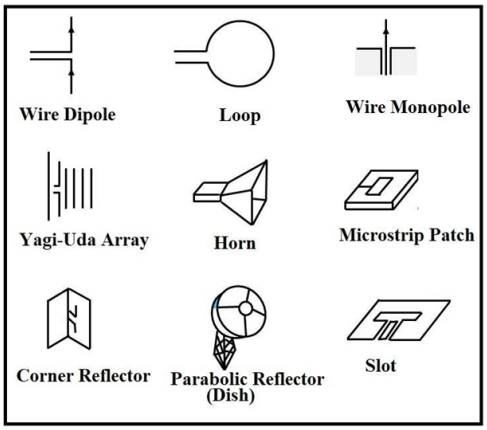

Figure I.1: Different types of antenna

I.2.2 The frequency of use

An antenna is generally employed with signals that are focused on a specific frequency at which it can most effectively transmit or receive the associated electromagnetic energy in its environment. The resonant frequency of an antenna is affected by its physical dimensions as well as any modifications made to it. A reduction of 3 dB establishes the minimum and maximum operational frequencies in relation to the antenna's fundamental resonance frequency; the range between these two frequencies defines the bandwidth. [1].

I.2.3 Antenna impedance

The connection between the voltage and the current flowing into an antenna is referred to as its impedance. This impedance is typically complex, consisting of a real component known as resistance and an imaginary component termed reactivity. This impedance is determined by [1]

$$Z = \frac{V}{I} = R_r + jX \tag{I.1}$$

I.2.4 Polarization of antenna

An antenna's polarization is actually the polarization of the light that it emits. It is defined by paying attention to how the vector $\vec{E}$ spreads, different polarizations following are reported in figure I.2.

I.2.4.1 Linear polarization

When the electrical field propagates in a steady direction over time, it is known to be a straight or linear polarization.

I.2.4.2 Circular polarization

When the electrical field describes a helix with a right section that circulates throughout time, the polarization of the electron is referred to as circular. A circle is produced when the extreme of $\vec{E}$ is projected onto an orthogonal layout. This circle can be described in terms of time in a sense of. On the other hand, one speaks of either right or left circulatory polarization.

I.2.4.3 Elliptic polarization

In this instance, the elongation of the vector describes an ellipse when projected into a plane perpendicular to the propagation. The right and left elliptic polarizations are distinguished, just as in the case of circulatory polarization.

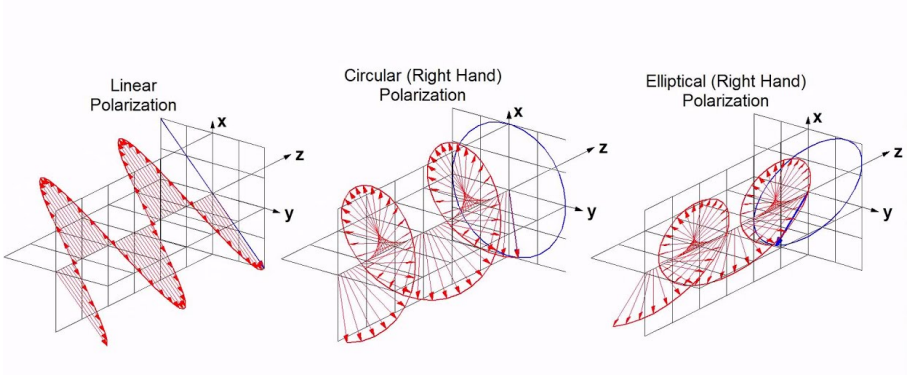

Figure I.2: Representation of different polarizations

I.2.5 Directivity

The manner in which an antenna concentrates its radiation in specific directions in space is referred to as its directivity. As illustrated in figure I.3, the power radiated in a particular direction, denoted as $P(\theta,\phi)$, is compared to the power that would be radiated by an isotropic source per unit solid angle. This comparison defines the antenna's directivity in the direction (θ,ϕ) [2]. In other words, the directivity $D(\theta,\phi)$ of an antenna in a specific direction (θ,ϕ) is defined as the ratio of the radiation intensity $U(\theta,\phi)$ in that direction to the radiation intensity that would be produced by an isotropic antenna emitting the same total power. Mathematically, this relationship is expressed as [3]:

$$D(\theta,\phi) = \frac{P(\theta,\phi)}{\frac{P_R}{4\pi}} = 4\pi\frac{P(\theta,\phi)}{P_R} \tag{I.2}$$

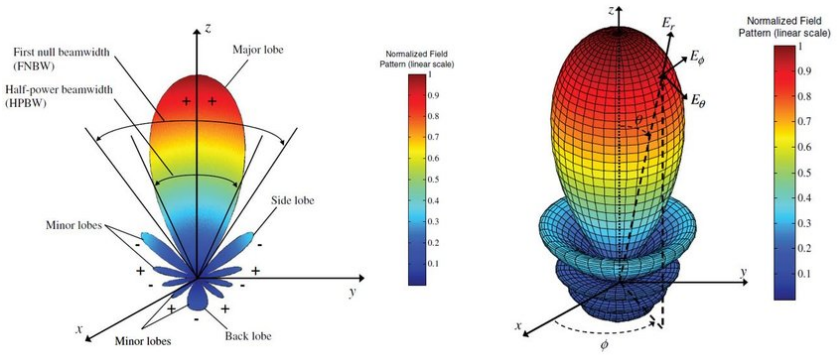

Figure I.3: An example of an antenna's radiation diagram

I.2.6 Gain

Antenna Gain is a key performance metric that quantifies how effectively an antenna directs or concentrates radio frequency energy in a particular direction. Antenna gain measures how well an antenna converts input power into radio waves directed in a specified direction. It is defined as the ratio of the radiation intensity in a given direction to the radiation intensity that would be produced if the power accepted by the antenna were radiated isotropically (equally in all directions).The relationship between antenna gain $G(\theta,\phi)$, directivity $D(\theta,\phi)$, and radiation efficiency η is given by the equation [4]:

$$G(\theta,\phi) = \eta \cdot G(\theta,\phi) \tag{I.3}$$

I.2.7 Efficiency

Antenna efficiency quantifies how effectively an antenna converts the power it receives into radiated electromagnetic energy. It is defined as the ratio of the power radiated by the antenna (P_R) to the total power accepted at its input terminals (P_A) [4]:

$$P_R = \eta \cdot P_A \quad \Rightarrow \quad \eta = \frac{P_R}{P_A} \tag{I.4}$$

Efficiency values range between 0 and 1, or 0% to 100%, with 1 (or 100%) indicating an ideal antenna that radiates all the power it receives without any losses.

I.3 Antenna arrays

I.3.1 Definition

An array of antennas is a collection of identical antennas (antennas, filagrees, cornets, patches, etc.) with the same orientation, arranged in a specific shape, and stimulated by an alimentation system to produce a specific type of radiation. The power radiated is greater because the resultant radiation is the superposition of the radiations from each

element. The radiating pattern of an antenna array is more precise than that of an single antenna system, and its gain and directivity are also significant. Because of these benefits, modern telecommunications systems use antenna arrays as emission and reception devices [5].

I.3.2 Type of antenna arrays

There are various geometric configurations of antenna networks that can be grouped as follows: linear, circular, and planar arrays, different polarizations following are reported in figure I.4 [5].

I.3.2.1 Linear array

A set of N elementary sources (aligned on a right) arranged along a specified axis and excited by a single alimentation system at an interface and N outputs is called a linear network. In the case of multi-frequency antennas, the feeding system with M inputs and N outputs can be viewed at the radiation level as the linear superposition of M subsystems to an input [6].

I.3.2.2 Circular array

A circular array is a network with radiating elements distributed around the edge of a circle and equals spaces. The horizontal plan is the one where network analysis is limited, and it is identified by polar coordinates (α, φ) [5].

I.3.2.3 Planar array

An antenna layout in a plan is called a planar array. The rectangular array plan is a generalization of the linear array design. The easiest case to put in equation is the one that is put in array according to a rectangular mesh of radiating $N \times M$. elements. The resulting rectangular array's path may vary depending on the array's two main axes [5].

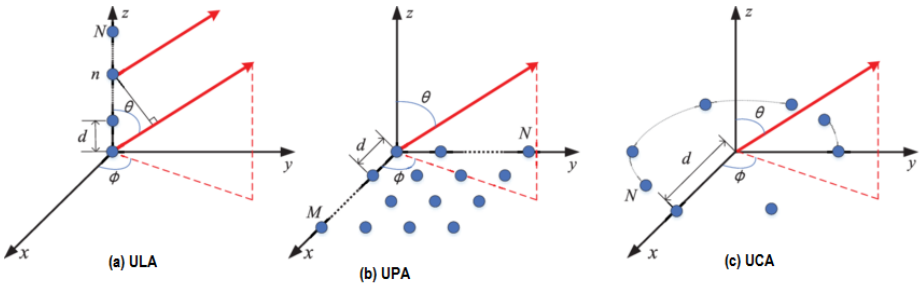

Figure I.4: Antenna Array Type Geometries

I.4 Smart antenna system

Smart antennas are based on adaptive beamforming. The idea is to use an antenna array and modify the excitation conditions of each radiating element in real time to alter the radiation pattern and adapt to a changing environment. This control is based on signal processing that requires a lot of computation time, and although there is much research and innovation in this field, this type of technique is not yet widely adopted in cellular networks and telecommunications standards. However, pressure to reduce costs, increasing constraints on capacity, coverage, throughput, and the number of existing systems on different frequencies are increasing the cost of antenna development and making the introduction of smart antennas increasingly attractive to operators [3].

I.4.1 Types of smart antenna

Basically, there are two main types of smart antennas [7]:

- A switchable beam smart antenna: This type uses analog circuits (switches) to modify the phase and amplitude of the excitations of the array elements. It is the simplest in terms of signal processing and circuit complexity.
- An adaptive array smart antenna: This type is largely digital. It adjusts its radiation pattern in real time based on spatial changes in the signal-to-noise ratio, or signal-to-interference ratio.

In the presence of low-level interference, both types of smart antennas provide significant gains over systems consisting of conventional antennas. However, when high-level interference is present, the ability to reject it is much better guaranteed by the adaptive array antenna than by the switchable beam or conventional antenna [8].

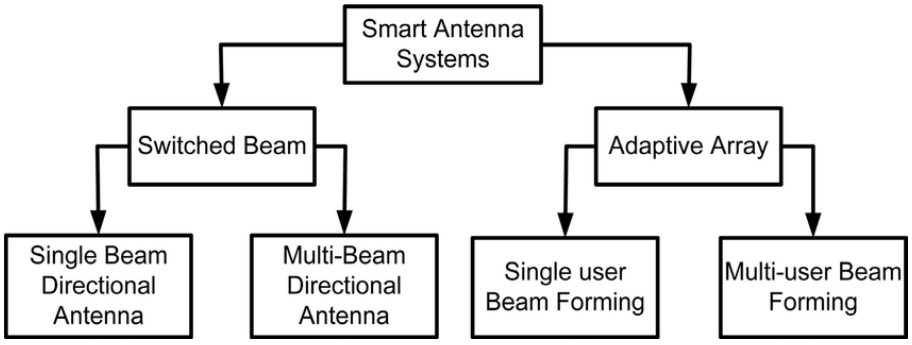

Figure I.5: Type of smart antenna

I.5 Structure of adaptive antenna system

This system consists of an antenna array connected to a real-time adaptive processor (a digital signal processing tool) that assigns weights to the signals incident on the array

elements in order to optimize the output signal according to predefined adaptive control algorithms, as shown in the figure below. An adaptive antenna array can therefore be defined as an array capable of modifying its radiation pattern, frequency response, and other parameters through an internal decision feedback loop during antenna operation . This type of smart antenna can dynamically combine different signals based on

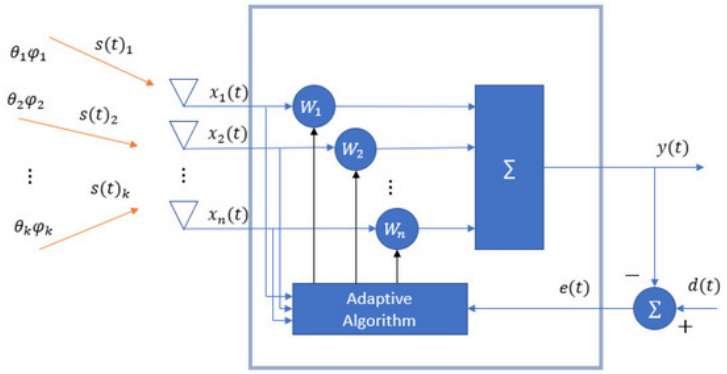

Figure I.6: Structure of adaptive antenna system

propagation conditions in order to concentrate power only in the direction of users [8].

I.6 Adaptive antenna functions

Adaptive antennas perform several key functions, two of the most important being Direction of Arrival (DoA) estimation and beamforming. These functions are integral to maximizing the performance of adaptive antenna systems in various applications, from wireless communications to radar systems. Here's an overview of each of these functions.

I.6.1 Direction of Arrival (DoA)

The smart antenna system determines the direction of arrival (DoA) of signals by employing various techniques, including MUSIC (MUltiple SIgnal Classification), ESPRIT (Estimation of Signal Parameters via Rotational Invariance Techniques), the Matrix Pencil method, or their derivatives [9]. These methods require the identification of the spatial spectrum of the antenna or sensor array, from which the DoA is derived by analyzing the peaks in this spectrum. Such computations demand significant processing power. The Matrix Pencil method is particularly effective for real-time applications, especially when dealing with correlated sources.

I.6.2 Beamforming

Adaptive beamforming is used for enhancing a desired signal while suppressing noise and interference at the output of an array of sensors. The aim of the adaptive beamforming is to optimize a collection of weight vectors to locate a directional source. There are different

methods in arriving at this optimization problem. Figure I.7 shows the structure of an adaptive beamformer. In applications where signal strength is unknown and is always present, application of linear constraints to the weight vector permits extensive control of the adaptive behavior of the beamformer[8].

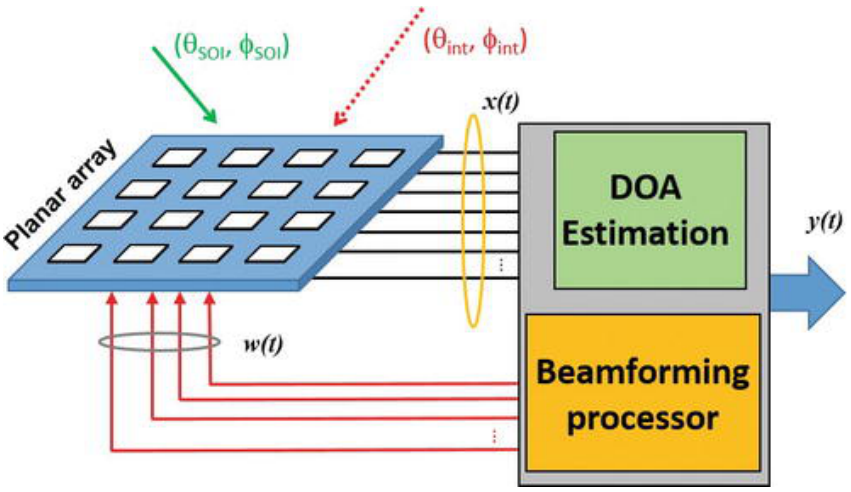

Figure I.7: adaptive antenna system

I.7 Advantage of adaptive antenna

The advantages of this system include

- Ability to track multiple users at the same time.
- Ability to continue distinguishing between the desired signal and the signal.
- The radiation pattern is dynamically optimized in real time.
- The radiation pattern of an adaptive system is more accurate than that of a switched-beam system.

I.8 Adaptive of antenna system application

These varied applications illustrate the essential function of adaptive antenna systems in enhancing performance across numerous sectors, including communication, navigation, safety, and exploration.

- Mobile Networks: adaptive antennas facilitate beamforming, which strengthens signal quality and extends coverage while minimizing interference, resulting in improved data rates and more dependable connections.
- Wi-Fi Networks: they enhance signal range, reduce interference, and elevate connection quality in densely populated areas by dynamically adjusting beam orientations.

- Signal optimization: by directing beams toward satellites and reducing interference from other sources, adaptive antennas ensure high-quality communication.

- Oil and Gas Exploration: these antennas improve the detection of seismic signals and enhance signal clarity in difficult environments.

- Smart cities: adaptive antennas bolster wireless communication among devices in urban settings by enhancing coverage and minimizing interference.

I.9 Angle of arrival estimation

Angle of Arrival (AoA), also known as Direction of Arrival (DoA), refers to the direction from which a radio frequency signal arrives at a receiver. In a typical setup, a single-antenna transmitter sends signals to a receiver equipped with an antenna array, forming a Single Input Multiple Output (SIMO) system. When the transmitted signal reaches the receiver from a distant source, it can be approximated as a planar wavefront (far-field condition). Due to the spatial separation of the antenna elements in the array, the signal arrives at each antenna at slightly different times, depending on the angle of incidence. These time differences lead to phase differences in the received signals across the antenna elements.By analyzing these phase differences, the system can estimate the AoA of the incoming signal. This estimation is crucial in applications such as radar, wireless communications, and localization systems [10]. An illustration of AoA estimation is presented in figure I.8.

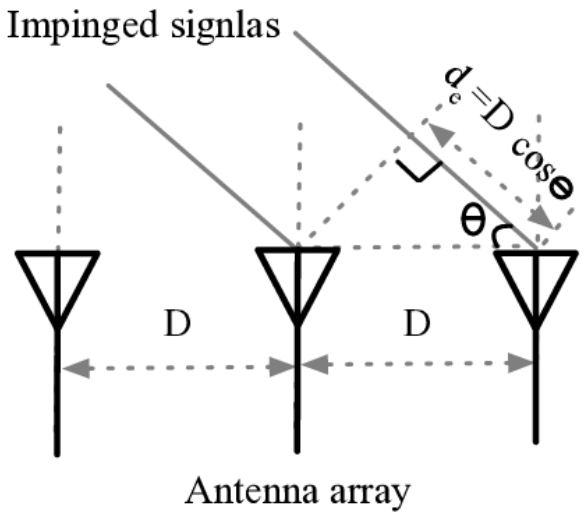

Figure I.8: Angle of arrival estimation

I.10 Conclusion

In wireless communications, adaptive antennas employ beamforming techniques to focus signals toward intended users, improving signal-to-noise ratios and reducing interference. This capability is crucial for technologies like 5G, where maintaining high data rates and reliable connections is essential. Adaptive antenna systems are transforming modern communication and sensing technologies by dynamically optimizing signal directionality and power. Through real-time beamforming, they enhance performance, reduce interference, and adapt to complex environments. Applications span from improving mobile communications and radar systems to advancing sonar capabilities and environmental monitoring, making them integral to next-generation technological advancements.

Chapter II

Direction of Arrival (DoA) estimation

II.1 Introduction

Direction of Arrival (DoA) estimation is a technique used to determine the direction from which a received signal is arriving at an array of sensors, such as microphones or antennas. This is a fundamental problem in various fields like telecommunications, radar systems, sonar, audio processing, and wireless communication. The goal of DoA estimation is to identify the angles or directions from which signals arrive, allowing systems to locate sources, enhance communication, or improve signal processing. In this context, DoA estimation requires complex signal processing from an array of sensors or antennas and the application of various techniques to obtain an accurate direction estimate. This process involves the use of advanced algorithms like MUSIC, Root MUSIC, CAPON, MIN-NORM, Root MIN-NORM, ESPRIT and propagation method(PM). which rely on spectral properties, as well as advanced processing techniques like beamforming and computational optimizations. In this chapter, we will describe several techniques used for DoA estimation, including classical methods such as antenna arrays and conventional beamforming, as well as more advanced methods like the MUSIC algorithm and optimization techniques.

II.2 Signal model

In this paper section, we introduce the general signal model that is considered for DoA estimation problem. For clarity sake, we consider a Uniform Linear Array (ULA) consists of M isotropic sensors; each two adjacent sensors are equally separated by a distance d.The array receives K narrow band plane waves S_k , $1 \leq k \leq K$, that come at distinct angles θ_k as illustrated in Figure II.1 [11].

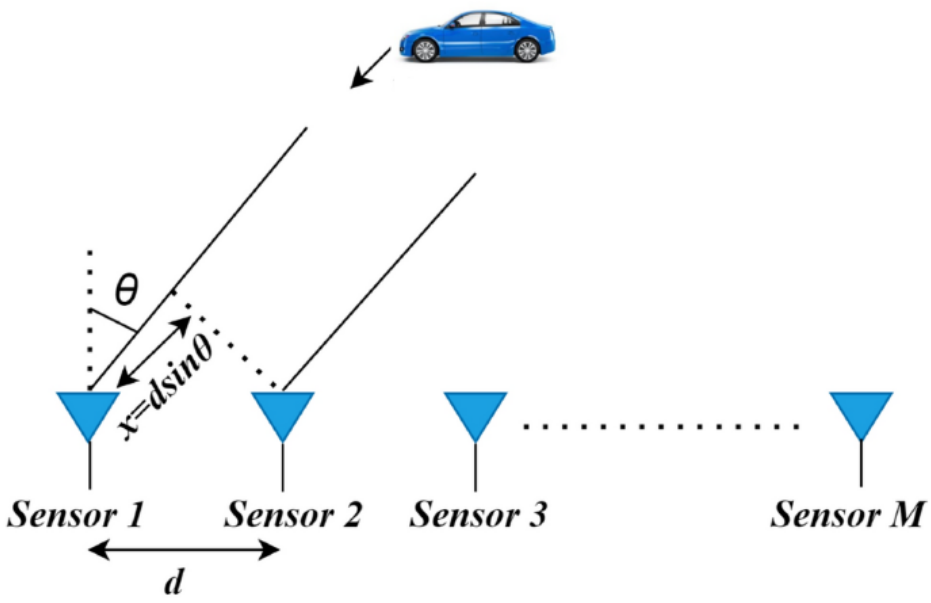

Figure II.1: System model for DoA estimation using a ULA of M sensors receiving K plane waves

The received signal $x(t)$ at any time t is a $M \times 1$ complex vector often written as:

$$x(t) = \sum_{k=0}^{K} a(\theta_k) s_k(t) + n(t) = A(\theta) S(t) + n(t) \tag{II.1}$$

where $A(\theta) = [a(\theta_1), a(\theta_2), \ldots, a(\theta_k)]$ is a $K \times M$ matrix containing the $M \times 1$ array steering vectors $a(\theta_k)$, $s(t) = [S_1(t), S_2(t), \ldots, S_k(t)]^T$ is the incident signals vector, and $n(t)$ is the Mcomplex noise vector modelled as a zero mean Gaussian with a variance σ^2. For an array of uniform linear geometry, the k^{th} antenna steering vector $a(\theta_k)$ corresponding to the angle of arrivals θ_k is given as[11]:

$$a(\theta_k) = [1, e^{2j(d/\lambda)sin\theta_k}, \ldots, e^{2j(M-1)(d/\lambda)sin\theta_k}]^T \tag{II.2}$$

where λ is the carrier wavelength and $[.]^T$ is the transpose operator.

The $M \times M$ covariance matrix R_{xx} of the received signal can be derived as [11]:

$$\begin{aligned} R_{xx} &= E\left[x(t)x^H(t)\right] \\ &= E\left[\left(A(\theta)S(t) + n(t)\right)\left(A(\theta)S(t) + n(t)\right)^H\right] \\ &= A(\theta)\, E\left[S(t)S^H(t)\right] A^H(\theta) + A(\theta)\, E\left[S(t)n^H(t)\right] \\ &\quad + E\left[n(t)S^H(t)\right] A^H(\theta) + E\left[n(t)n^H(t)\right] \\ &= AR_S A^H + R_N \end{aligned} \tag{II.3}$$

where $R_S = E[S(t)S^H(t)]$ is the signal covariance matrix, and $R_N = E[n(t)n^H(t)]$ is the noise covariance matrix. $E[.]$ and $(.)^H$ stand for the expectation and the Hermitian transpose,

respectively.

Under the uncorrelated signal and noise assumption and the zero-mean noise property, the expectation of the cross-term matrices ($R_{SN} = E[S(t)n^H(t)]$ and $R_{NS} = E[n(t)S^H(t)]$) between the signal and noise vectors is zero.

Notice that R_S is a diagonal matrix when the signals are uncorrelated, and in this case its rank is equal to the number of sources K. The matrix R_S is non-diagonal and non- singular when the signals are partially correlated. The matrix R_S is non-diagonal but singular when some signals are fully correlated (or coherent) (Shan et al., 1985), and in this case R_S has a rank degradation ($\text{rank}(R_S) < K$)[11].

Under other mathematical matrix writing, the expanded form of the covariance matrix of (II.3) gives a $M \times M$ coherent data covariance matrix which can be expressed as:

$$R_{xx} = \begin{bmatrix} r_{xx}(1,1) & r_{xx}(2,2) & \cdots & r_{xx}(1,M) \\ r_{xx}(2,1) & r_{xx}(2,2) & \cdots & r_{xx}(2,M) \\ \vdots & \vdots & \ddots & \vdots \\ r_{xx}(M,1) & r_{xx}(M,2) & \cdots & r_{xx}(M,M) \end{bmatrix} \tag{II.4}$$

Generally, the true spatial covariance matrix is unknown in practice, and in theory, an estimated sample data covariance matrix for L snapshots should be defined as follows:

$$\hat{R}_{xx} = \frac{1}{L}\sum_{l=1}^{L} x(l)x^H(l) \tag{II.5}$$

Once the composite array covariance matrix is defined, the most of narrow band methods can be applied to generate a DOA estimation using this matrix. Accordingly, Eigen-Value Decomposition (EVD) on the said matrix must be necessary for all approaches belonging to the DOA[11].

The EVD of $\hat{R}_{xx}$ can be then expressed as:

$$R_{xx} = \sum_{i=1}^{M} \omega_i e_i e_i^H = V_S \Omega_S V_S^H + V_N \Omega_N V_N^H \tag{II.6}$$

where ω_i is the i^{th} eigenvalue associated with the i^{th} eigenvector e_i , and $\Omega = diag(\omega_1, \omega_2, \ldots, \omega_M)$ is a diagonal matrix containing the eigenvalues.

If the M eigenvalues of the matrix $\hat{R}_{xx}$ are sorted from the largest to the smallest which is equal to the noise variance σ^2 , the eigenvectors corresponding to the biggest eigenvalues span the signal subspace V_S which is orthogonal to the noise subspace V_S. This last is spanned by the other eigenvectors corresponding to the smaller eigenvalues[11].

II.3 Coherence between signals

In the context of signal processing, coherence refers to a statistical measure utilized to analyze the relationship between two signals or data sets. It is frequently employed to assess the power transfer from the input to the output of a linear system. When the signals exhibit ergodicity and the system function is linear, coherence can also be used to infer the causality between the input and output. Considering two zero-mean random processes x and y,the coherence between x and y at the frequency of interest f is defined by [12]:

$$\rho_{xy}^2(f) = \frac{|S_{xy}(f)|^2}{S_{xx}(f) \cdot S_{yy}(f)} \tag{II.7}$$

where $S_{xy}(f)$ is the cross-spectral density between the two processes x and y (i.e. the Fourier transform of the cross-correlation function $R_{xy}(\tau)$):

$$S_{xy}(f) = \int_{-\infty}^{+\infty} R_{xy}(\tau) e^{-i2\pi ft}\, d\tau \tag{II.8}$$

with

$$R_{xy}(\tau) = E\left[x(t)\, y(t-\tau)\right] \tag{II.9}$$

where $E[.]$ is the expectation operator, i.e. for a process s, $E(s)$ is the average value of $s(t)$ over an infinite period of time.

Since S_{xy} is a scalar product, the Schwartz inequality guarantees that $\rho_{xy}(f)$ takes its values between 0 and 1.
It can be shown that $\rho_{xy}(f)$ is roughly equal to the correlation coefficient between the components of x and y at frequency f. Furthermore, if $\rho_{xy}(f)$ is close to 1 for all frequencies, then x can be approximated by a linear time-invariant transformation of y [12].

II.4 Correlation between signals

One benefit of utilizing a microphone array for recording is the capacity to examine the correlation among various channels. In this context, the autocorrelation functions $R_{xx}(\tau)$ and $R_{yy}(\tau)$, along with the cross-correlation function $R_{xy}(\tau)$ for the two signals $x(t)$ and $y(t)$, are particularly valuable [13].

$$R_{xx}(\tau) = \frac{1}{T} \int_0^T x(t)\, x(t+\tau)\, dt \tag{II.10}$$

$$R_{yy}(\tau) = \frac{1}{T} \int_0^T y(t)\, y(t+\tau)\, dt \tag{II.11}$$

$$R_{xy}(\tau) = \frac{1}{T} \int_0^T x(t)\, y(t+\tau)\, dt \tag{II.12}$$

When dealing with digital data, equations (II.10) - (II.12) can be approximated as

$$\hat{R}_{xx}(r\Delta t) = \frac{1}{N-r}\sum_{n=1}^{N-r} x(n)\,x(n+r) \tag{II.13}$$

$$\hat{R}_{yy}(r\Delta t) = \frac{1}{N-r}\sum_{n=1}^{N-r} y(n)\,y(n+r) \tag{II.14}$$

$$\hat{R}_{xy}(r\Delta t) = \frac{1}{N-r}\sum_{n=1}^{N-r} x(n)\,y(n+r) \tag{II.15}$$

where $r = 0,1,2,\ldots,m$ with $m < N$. Another quantity of interest is the cross-correlation coefficient function $\rho_{xy}(\tau)$,given by:

$$\rho_{xy}(\tau) = \frac{R_{xy}(\tau)}{\sqrt{R_{xx}(0)\,R_{yy}(0)}} \tag{II.16}$$

which can be approximated from equations (II.13) – (II.15) by;

$$\hat{\rho}_{xy}(r\Delta t) = \frac{\hat{R}_{xy}(r\Delta t)}{\sqrt{\hat{R}_{xx}(0)\,\hat{R}_{yy}(0)}} \tag{II.17}$$

This quantity always satisfies $-1 \leq \rho_{xy}(\tau) \leq 1$. Since the cross-correlation coefficient is a normalized quantity, it is ideal for use in comparing different waveforms.

II.5 Coherent and non-coherent signals

- In non-coherent processing, the resolution capability of the array is limited, compared to coherent processing, since the largest available covariance lag corresponds to the largest sub-array. Whereas, in coherent processing, the largest available covariance lag corresponds to the array aperture [14].

- The non-coherent processing scheme is more suitable for decentralized processing than the coherent processing one, since each sub-array can act as a decentralized processing node which computes the local covariance matrix of the sub-array and sends it to the Coherent Processing (PC). Whereas, in coherent processing, the computation of the cross-sub-array covariance matrices requires either sending the raw measurement to the PC or the use of the averaging consensus (AC) protocol, i.e., it involves a much larger communication overhead [14].

II.6 DoA estimation techniques

The received signals from the sensor array are used to identify the incoming signal directions. There are various algorithms that are able to find the signal directions which can be classified into three categories: classical-algorithms, subspace-based algorithms and maximum likelihood based algorithms.

II.6.1 MUSIC

MUSIC stands for Multiple Signal Classification. It had been firstly presented by Schmidt . It is an algorithm to estimate the direction of the source. MUSIC is mainly dependent on the correlation matrix of the data and the ability to extract the signal and noise eigenvectors from input correlation matrix. It works only with incoherent sources. The steps for MUSIC algorithm can be simplified as follows. The antenna array input signal is expressed as [15]:

$$x(t) = As(t) + n(t) \tag{II.18}$$

where $s(t)$ is the original signal from the d sources :

$$s(t) = [S_1(t), S_2(t), \ldots, S_d(t)]^T \tag{II.19}$$

$n(t)$ is the channel noise for M element array:

$$n(t) = [n_1(t), n_2(t), \ldots, n_M(t)]^T \tag{II.20}$$

The $x(t)$ signal received by the array antenna with M elements can be defined by:

$$x(t) = [x_1(t), x_2(t), \ldots, x_d(t)]^T \tag{II.21}$$

$$A = [a(\mu_1), a(\mu_2), \ldots, a(\mu_d)] \tag{II.22}$$

where A is the array steering vector for d sources and have different structure according to the array configuration and the spatial frequency $a(\mu_i)$. Here the uniform linear array is assumed, thus the spatial frequency and steering vector are given by :

$$\mu_i = \frac{-2\pi}{\lambda} \Delta \sin\theta_i \tag{II.23}$$

$$a(\mu_i) = [1, e^{j\mu_i}, e^{j2\mu_i}, \ldots, e^{j(M-1)\mu_i}] \tag{II.24}$$

where θ is the angle of arrival, and Δ is the separation distance between array elements. Substituting equation (II.24) in equation (II.22), the structure of A matrix corresponding

to spatial frequency is given by :

$$\mathbf{A} = \begin{bmatrix} 1 & 1 & \cdots & 1 \\ e^{j\mu_1} & e^{j\mu_2} & \dots & e^{j\mu_d} \\ e^{j2\mu_1} & e^{j2\mu_2} & \dots & e^{j2\mu_d} \\ \vdots & \vdots & \ddots & \vdots \\ e^{j(M-1)\mu_1} & e^{j(M-1)\mu_2} & \dots & e^{j(M-1)\mu_d} \end{bmatrix} \tag{II.25}$$

The input covariance matrix R_{xx} can be written as :

$$R_{xx} = AR_{ss}A^H + \sigma_N^2 I_M \tag{II.26}$$

where R_{xx} is the signal correlation matrix,σ_N^2 is the noise common variance, and I_M is the identity matrix of rank M. The covariance matrix R_{xx} will have M eigenvalues by averaging over the number of snapshot(N).

$$R_{xx} = \frac{1}{N}\sum_{n=1}^{N} x_n x_n^H \tag{II.27}$$

The covariance matrix R_{xx} will have M eigenvalues.The matrix $AR_{ss}A^H$ is positive definite with rank d. Hence, the smallest $(M-d)$ eigenvalues of R_{xx} represent the noise and should equal to the noise variance σ_N^2. Their corresponding eigenvectors V_n are orthogonal to the steering vector of the input signal $a(\theta)$. Thus, knowing these two values, the MUSIC spectrum is constructed to find the orthogonal points (maximum peaks) which represent the desired angles as [15] :

$$P_{\text{MUSIC}}(\theta) = \frac{1}{a(\theta)^H V_n V_n^H a(\theta)} \tag{II.28}$$

Where V_n is the noise subspace eigenvectors and $a(\theta)$ is the steering vectors corresponding to signal components as in equation (II.24). The peaks of this spectrum represent the required angles of arrival [15].

II.6.2 ROOT-MUSIC

This algorithm had been introduced as an improvement of above mentioned MUSIC algorithm by Barabell .Using the MUSIC spectrum, the root of the polynomial is used to estimate the angles of arrival. This algorithm is more practical, since the results are given in a numerical format instead of spectrum plotting in MUSIC algorithm. The algorithm can be summarized by the following steps [15] :

- Estimation of the covariance matrix R_{xx} by weighting over number of snapshots as in equation (II.27) .

- Extraction of the smallest eigenvalues of R_{xx} and their corresponding eigenvectors to estimate noise subspace.
- Generation of the polynomial from the MUSIC spectrum using the following equation:

$$P_{\text{MUSIC}}(\theta) = \frac{1}{j(\theta)} = \frac{1}{a^H(\theta)V_nV_n^Ha(\theta)} = 0 \tag{II.29}$$

  where the steering vector was defined previously as in equation (II.24) and it depends on the spatial frequency μ. Thus, calculating the root for the polynomial will give the values for the variable μ. Here the uniform linear array was assumed and μ is defined by equation (II.23) [15] .
- The zeros of the polynomial are calculated in term of $(N-1)$ pairs within the unit circle.
- The closest d roots to unit circuit are then selected. Finally, the values of the angles of arrival are directly calculated using the following formula:

$$\theta = \sin^{-1}\left[\frac{\lambda\mu}{2\pi\Delta}\right] \tag{II.30}$$

II.6.3 CAPON

Capon algorithm, which is introduced by J. Capon, is a conventional spectral-based method to improve the resolution of Bartlett algorithm . The main idea of Capon algorithm is to minimize the received power of the incoming signal in all direction while maintaining a unity gain in 'look direction' [8], [16].

The constraint imposed on this algorithm is given as:

$$\min_{\omega} \ \omega^H R_{xx}\omega \quad subject \quad to \quad \omega^H a(\theta) = 1 \tag{II.31}$$

where ω is the weight to be calculated. Applying Lagrange optimization method to the constraint yields the optimised weight:

$$\omega = \frac{R_{xx}^{-1}a(\theta)}{a(\theta)^H R_{xx}^{-1}a(\theta)} \tag{II.32}$$

Using the optimized weight, the spatial power spectrum of Capon is given as [17]:

$$P_{\text{Capon}}(\theta) = \frac{1}{a(\theta)^H R_{xx}^{-1}a(\theta)} \tag{II.33}$$

II.6.4 MIN-NORM

The Min-Norm algorithm was initially proposed for frequency analysis and antenna processing. It facilitates the estimation of the directions of arrival for a known number of

signals based on measurements taken from an antenna array. This approach involves identifying a minimum norm vector that lies within the noise subspace to locate the peaks in the pseudo-spectrum . In comparison to the reference method MUSIC, the Min-Norm technique defines the pseudo-spectrum of a vector x from the noise subspace that possesses a minimal norm. The computation of the minimum norm vector x adheres to three specific constraints [8]:

- x belongs to the noise subspace V_n, and is therefore orthogonal to the projector V_s onto the signal subspace v_M defined by:

$$V_s = [v_1, v_2, \ldots, v_M] \quad , \quad V_s^H x = 0 \tag{II.34}$$

- The first element of x is equal to 1.

- The Euclidean norm of x is at its minimum.

Finally, since the Min-Norm method is a spectral search technique, we define the formula for the associated pseudo-spectrum:

$$P_{\text{Min-Norm}}(\theta) = \frac{1}{|a^H(\theta) V_n^H u_1|^2} \tag{II.35}$$

II.6.5 ROOT-MIN NORM

The same principles that are applied to root-MUSIC can also be utilized in the Min-Norm method to develop a polynomial version known as root-Min-Norm. We can express this as follows [8], [18]:

$$P_{\text{Min-Norm}}(\theta) = \frac{1}{|a^H(\theta) V_n V_n^H u_1|^2} = \frac{1}{|a^H(\theta) C u_1|^2} \tag{II.36}$$

In this context, u_1 represents the Cartesian basis vector (the first column of the identity matrix $N \times N$), which contains all zeros except for the first element, which is equal to one. The matrix $C = V_n V_n^H$ is a Hermitian projection matrix, and V_n denotes the eigenvectors of the noise subspace, while $a(\theta)$ signifies the directional vector. When the Cartesian basis vector is multiplied by the Hermitian matrix, it results in a column vector that corresponds to the first row of the matrix C. The column vector derived from the first column of C is expressed as $C_1 = [C_{11} C_{12}, \ldots C_{1N}]$, where the index 1 indicates the first column [8].

We can substitute this in the equation (II.36):

$$P_{\text{min-norm}}(\theta) = \frac{1}{|a^H(\theta) c_1|^2} = \frac{1}{|a^H(\theta) c_1 c_1^H a(\theta)|^2} \tag{II.37}$$

II.6.6 ESPRIT

Estimation of Signal Parameter Rotation Invariance Technique is another subspace based algorithm, based on exploiting the rotation invariance in the signal subspace. This subspace is created by dividing a M element array in two identical sub arrays of size S in a translational invariance structure. Figure II.2 shows a translational structure of an four element array Array-2 is shifted by a distance d from array-1 to create the translational structure[19].

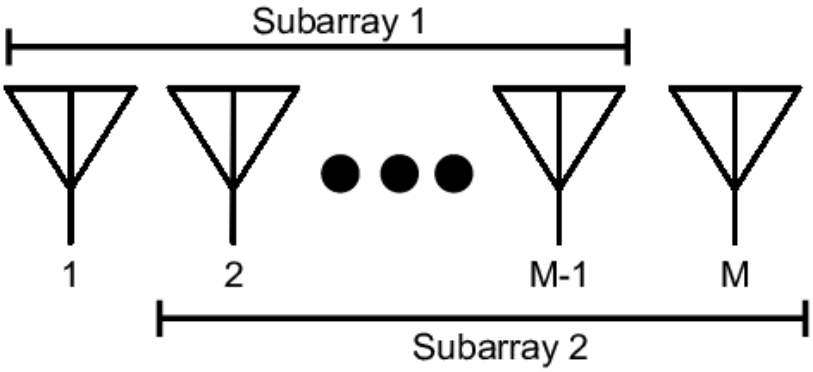

Figure II.2: Sub-array structure

The output of the two sub-arrays are given by

$$x_1(t) = A(t) + n_1(t)$$
$$x_2(t) = A\Phi(t) + n_2(t)$$

where $\Phi \in \mathbb{C}^{K\times K}$ is a diagonal matrix called the rotation operator and K is the number of sources,

$$\Phi = \text{diag}\left\{e^{-j\frac{2\pi}{\lambda}d\sin(\theta_1)},\ e^{-j\frac{2\pi}{\lambda}d\sin(\theta_2)},\ \ldots,\ e^{-j\frac{2\pi}{\lambda}d\sin(\theta_K)}\right\} \tag{II.38}$$

Now we can estimate the correlation matrices in the two sub-arrays as:

$$R_{xx11} = \mathbb{E}\left\{x_1(t)x_1^H(t)\right\}$$
$$R_{xx22} = \mathbb{E}\left\{x_2(t)x_2^H(t)\right\}$$

After eigen-decomposing R_{11} and R_{22} , we get the two signal subspaces : V_{S1} and V_{S2}. Defining a $2K \times 2K$ matrix C from the two subspaces such that:

$$C = \begin{bmatrix} V_{S1}^H \\ V_{S2}^H \end{bmatrix} \begin{bmatrix} V_{S1} & V_{S2} \end{bmatrix} = V_C \Lambda V_C^H \tag{II.39}$$

V_C can be obtained by eigen value decomposition of C such that $\lambda_1 \geq \lambda_2 \geq \ldots \geq \lambda_K$ and

$\Lambda = \text{diag}\{\lambda_1, \lambda_2, \ldots, \lambda_K\}$.

$$V_C = \begin{bmatrix} V_{11} & V_{12} \\ V_{21} & V_{22} \end{bmatrix} \tag{II.40}$$

The rotation operator is estimates as:

$$\Phi = -V_{12} V_{22}^{-1} \tag{II.41}$$

From K eigenvalues of Φ, the angles of arrival can be estimated [19]

$$\theta_i = \sin^{-1}\left(\frac{\arg(\lambda_i)}{2\pi d}\right) \tag{II.42}$$

II.6.7 Propagation Method

The Propagator Method (PM) operates under the assumption that the number of incoming signals is fewer than the number of antenna elements (L < M), with L needing to be predetermined. One of the key benefits of this approach is that it does not require the decomposition or inversion of the covariance matrix (CM). Furthermore, it is suitable for various array configurations and demonstrates high estimation accuracy. Consequently, it is regarded as having lower complexity in comparison to the MUSIC method, which necessitates an eigen decomposition of the CM. However, this technique is primarily effective in environments with white Gaussian noise, and its performance significantly declines in the presence of nonuniform colored noise. The core concept of the Propagator method involves partitioning the CM into two sub-matrices, as outlined below [20]:

$$R_{xx} = \begin{bmatrix} R_1 \\ R_2 \end{bmatrix} \quad \text{with} \quad \begin{cases} R_1 \in \mathbb{C}^L \\ R_2 \in \mathbb{C}^{M-L} \end{cases} \tag{II.43}$$

where R_1 and R_2 are matrices with size $(L \times M)$ and $(M - L \times M)$, respectively. By considering R_1 is a non-singular matrix, the propagator may be defined as a unique linear operator $\mathscr{P}$ of $\mathbb{C}^{M-L}$ into $\mathbb{C}^L$. In the noiseless system, the propagator is defined as:

$$R_2 = \mathscr{P}^H R_1 \tag{II.44}$$

However, when the environment is noisy, the LMS method is used to estimate $\mathscr{P}$ as expressed below,

$$\mathscr{P} = (R_1^H R_{xx})^{-1} R_1^H R_2 \tag{II.45}$$

Next, we need to construct a V matrix, such that

$$V = \begin{bmatrix} \mathscr{P} & -\mathbf{I}_{M-L} \end{bmatrix} \tag{II.46}$$

$\mathbf{I}_{M-L}$ is the identity with dimension$(M-L)\times M$. The spatial spectrum of the propagator method is expressed in the next formula:

$$P_{\mathrm{PM}}(\theta) = \frac{1}{\|a(\theta,\phi)V\ \|^2} \tag{II.47}$$

II.7 Techniques used for overcome the correlation and coherency

In Direction-of-Arrival (DoA) estimation, the main goal is to estimate the angle at which a signal arrives at a sensor array. However, challenges arise when signals are correlated or coherent, leading to difficulties in accurate DoA estimation [21]. These issues often arise due to multi-path propagation, interference, or the presence of multiple sources that are highly correlated. To overcome these challenges, several techniques have been developed.

II.7.1 Spatial Smoothing

For DoA estimation of coherent signals, spatial-smoothing technology is an effective de-coherence method. The basic idea is to divide the uniform linear array into multiple overlapping sub-arrays with the same number of array elements. The covariance matrix of each sub-array is summed and averaged, to obtain the rank recovered matrix [22]. The *ULA* is divided into L sub-arrays. Each sub-array has P elements, $P = M+1-L$, and the spatial-smoothing diagram is shown in Figure II.3 .

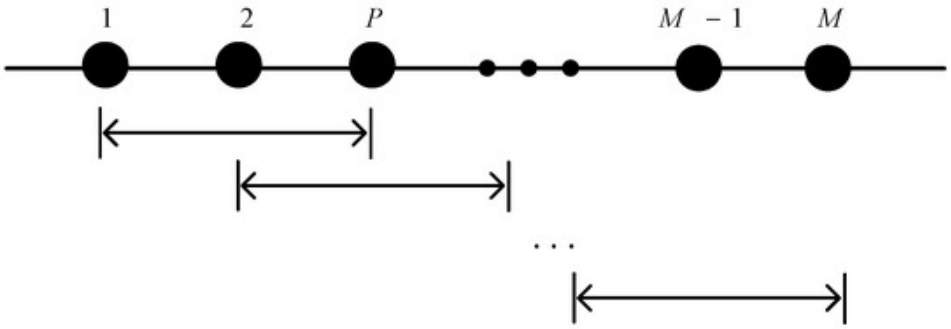

Figure II.3: Spatial-smoothing diagram

Taking the first sub-array as the reference array, the received data of the i^{th} forward-smoothed sub-array are expressed as:

$$x_i(t) = [x_i(t), x_{i+1}(t), \ldots, x_{i+P-1}(t)]^T \tag{II.48}$$

According to (II.48), the covariance matrix of the i^{th} sub-array forward-smooth receiving data is calculated:

$$R_{ii} = \frac{1}{N}\sum_{n=1}^{N} x_i x_i^H \tag{II.49}$$

After forward smoothing L times, the covariance matrix of the array receiving data is expressed as:

$$R^f = \frac{1}{L}\sum_{i=1}^{L} R_{ii} \tag{II.50}$$

Because there is a conjugate-reciprocal-invariant relationship between the forward-smoothing covariance matrix and the backward-smoothing covariance matrix, the backward-smooth covariance matrix $\bar{R}_{ii}$ of the i^{th} sub-matrix can be expressed as:

$$\bar{R}_{ii} = JR_{ii}^{*}J \tag{II.51}$$

where the superscript $()^*$ denotes the complex conjugate operation and J is a commutative matrix with order-counter-diagonal elements of 1 and the remaining elements of 0. Therefore, after backward smoothing L times, the covariance matrix of the array receiving data is expressed as

$$R^b = \frac{1}{L}\sum_{i=1}^{L} \bar{R}_{ii} \tag{II.52}$$

Based on (II.50) and (II.52), the spatial-smoothing covariance matrix is expressed as

$$R^{fb} = \frac{1}{2}(R^f + R^b) = \frac{1}{2L}\sum_{i=1}^{L}(R_{ii} + \bar{R}_{ii}) \tag{II.53}$$

The eigenvalue decomposition is performed on (II.53), to obtain the corresponding noise subspace and then it is substituted into (II.28) for the spectral-peak search, to obtain the DoA estimation value. The traditional spatial-smoothing algorithm does not use the cross-correlation covariance matrix between sub-arrays. Only the autocorrelation covariance matrix of a single sub-array is used, and the received data of the array are not fully utilized. Therefore, an improved spatial-smoothing algorithm is proposed in this paper, which can make full use of the array receiving data and can be directly applied to the signal subspace. When the incident signal is coherent, there is only one signal eigenvalue λ_1 in the covariance matrix R, so the signal subspace contains only one eigenvector, u_1. At this time, the signal covariance matrix V_s is expressed as

$$V_s = \lambda_1 \mathbf{u}_1 \mathbf{u}_1^H \tag{II.54}$$

The signal feature vector u_1 is divided into L sub-arrays; then, the $i-th$ sub-array forward-smooth autocorrelation matrix V_{ii} is expressed as

$$V_{ii} = z_i z_i^H \tag{II.55}$$

where z_i is the $i-th$ sub-matrix of u_1. According to (II.51), we know that the i^{th} sub-matrix backward-smooth autocorrelation matrix $\tilde{V}_{ii}$ is

$$\tilde{V}_{ii} = JV_{ii}^{*}J \tag{II.56}$$

According to (II.55) and (II.56), the rank recovery matrix R_1 is constructed by using all the forward-smoothing and backward-smoothing autocorrelation matrices:

$$R_1 = \frac{1}{2L}\sum_{i=1}^{L}\sum_{j=1}^{L}\left(V_{ii}V_{jj} + \tilde{V}_{ii}\tilde{V}_{jj}\right) \tag{II.57}$$

Similarly, the forward-smoothed cross-correlation matrix Vij of the ith and jth sub-matrices of u_1 can be expressed as

$$V_{ij} = z_i z_j^{H} \tag{II.58}$$

Therefore, the backward-smoothed cross-correlation matrix $\tilde{V}_{ij}$ between the ith and jth sub-matrices is defined as

$$\tilde{V}_{ij} = JV_{ij}^{*}J \tag{II.59}$$

According to (II.57) and (II.58), the rank recovery matrix R_2 is constructed by using all the cross-correlation matrices:

$$R_2 = \frac{1}{2L}\sum_{i=1}^{L}\sum_{j=1}^{L}\left(V_{ij}V_{ji} + \tilde{V}_{ij}\tilde{V}_{ji}\right) \tag{II.60}$$

Therefore, the covariance matrix R_{IM} of the improved spatial-smoothing technique is expressed as

$$R_{\mathrm{IM}} = R_1 + R_2 = \frac{1}{2L}\sum_{i=1}^{L}\sum_{j=1}^{L}\left\{\left(V_{ii}V_{jj} + \tilde{V}_{ii}\tilde{V}_{jj}\right) + \left(V_{ij}V_{ji} + \tilde{V}_{ij}\tilde{V}_{ji}\right)\right\} \tag{II.61}$$

Eigenvalue decomposition is performed on (II.61), and then DoA estimation of coherent signals is realized by combining the MUSIC algorithm. Compared to the traditional algorithm, this method makes full use of the information of the signal subspace and has better noise-suppression ability [22].

II.7.2 Approaches based on Toeplitz matrices reconstruction

The decorrelation Toeplitz technique takes the coherent array covariance matrix R_{xx} to average the oblique diagonal elements of its lower triangular part. The elements $v_a(i)$ of the $M \times 1$ obtained vector can be calculated according to the following expression [11]:

$$v_a(i) = \frac{1}{M-i+1}\sum_{m=1}^{M-i+1} r_{xx}(m, m+i-1), \quad i = 1,2,\ldots,M \tag{II.62}$$

Hence, we can define a resulting $M \times M$ Toeplitz matrix T_{va} as:

$$T_{va} = \begin{bmatrix} v_a(1) & v_a(2) & \cdots & v_a(M) \\ v_a(2)^* & v_a(1) & \cdots & v_a(M-1) \\ \vdots & \vdots & \ddots & \vdots \\ v_a(M)^* & v_a(M-1)^* & \cdots & v_a(1) \end{bmatrix} \tag{II.63}$$

II.7.2.1 Combined Averaging-Toeplitz Min-Norm Algorithm

In theory, and within specific limitations, the Min-Norm algorithm is capable of achieving high resolution in the estimation of arrival directions. However, its shortcomings are evident when estimating signals with low signal-to-noise ratios (SNR) or when dealing with highly correlated or coherent signal sources. To address these challenges, this subsection introduces and elaborates on a novel algorithm that relies on a transformation of the estimated Toeplitz spatial covariance matrix. We have developed an initial min-norm DoA scheme utilizing a decorrelation technique. This technique involves averaging to create the components of a Toeplitz matrix. The algorithm introduced in this context is referred to as the Averaging Toeplitz for Min-Norm (AT-MN)[11]. The last new Toeplitz matrix T_{va} (II.63) is mainly reconstituted from the averages of diagonals of coherent array covariance matrix R_{xx} . Thus, the superdiagonal entries of the reconstructed matrix T_{va} are a mixture of independent DoA terms and biased terms. This means that every column or row has one entry containing biased terms which leads to resolve the coherence signals problem, but it can result lower accuracy in the DoA estimation[11]. Currently, we utilize the decorrelated Toeplitz matrix T_{va} in place of the covariance matrix R_{xx} for the min-norm algorithm to determine the DoA. The matrix T_{va} can still be characterized by its eigenvalues and eigenvectors as follows [11]:

$$T_{va} = \sum_{i=1}^{M} \omega_{1i} e_{1i} e_{1i}^H = V_{1S} \Omega_{1S} V_{1S}^H + V_{1N} \Omega_{1N} V_{1N}^H \tag{II.64}$$

where V_{1S} and V_{1N}^H are the new signal and noise subspaces, respectively.
The derivation of the updated AT-MN spectrum expression relies on the computation of a novel min-norm vector u_{11} that resides within the noise subspace V_{1N}, which is obtained from the decomposition of the Toeplitz matrix. Consequently, this spectrum is constructed as follows [11]:

$$P_{\text{AT-MN}}(\theta) = \frac{1}{|a^H(\theta) V_{1N} V_{1N}^H u_{11}|^2} \tag{II.65}$$

The AT-MN algorithm is categorized as a spectral-based method. The function outlined in equation (II.65) can be utilized to generate the AT-MN spectrum, with the positions of the distinct highest peaks serving as the estimated DoAs[11]. For simple clarity, the first

proposition is summarised in the steps of the Algorithm 1, while the flowchart illustrating this proposal for estimating DoA of coherent signals is displayed in Figure II.4.

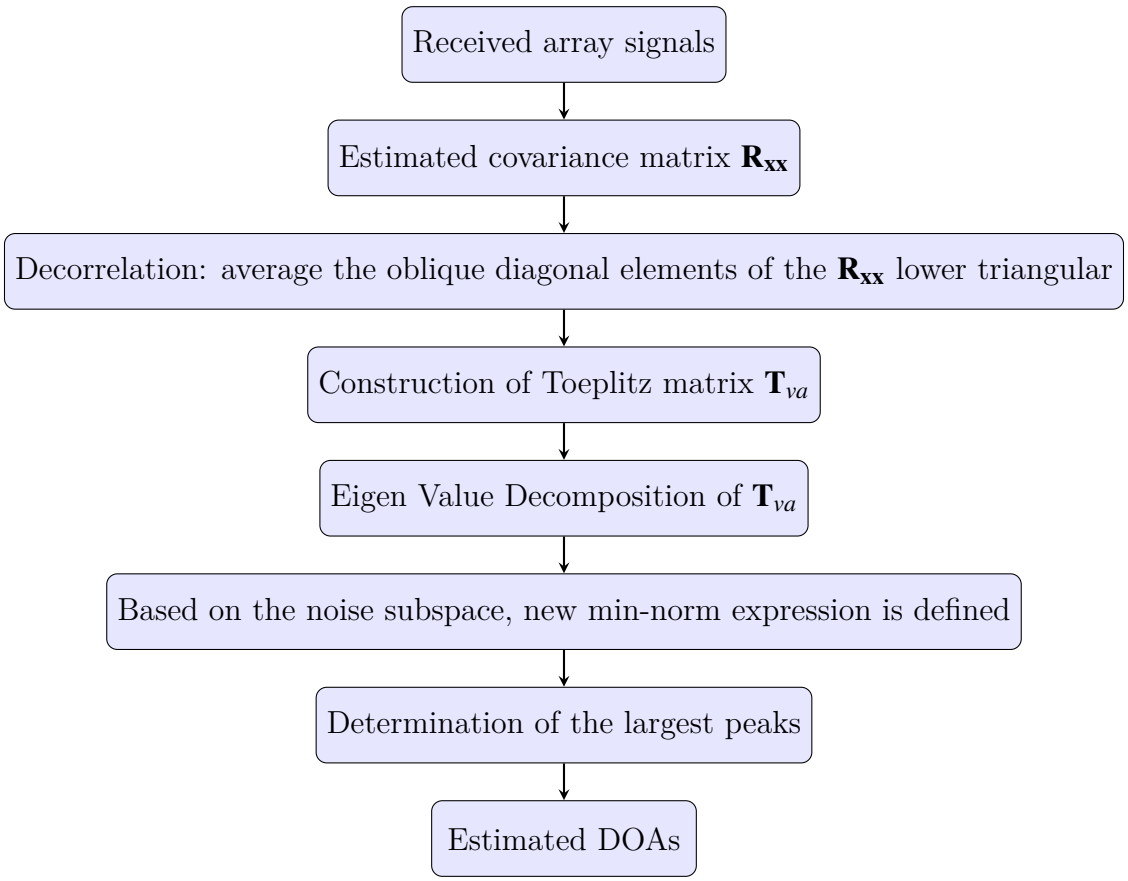

Figure II.4: The flow chart of our first proposed algorithm

Algorithm 1: AT-MN for estimating DOA of coherent signals

Step 1:	Estimate the autocorrelation matrix of receiving signals using equation (II.5)
Step 2:	Compute the average of oblique diagonal elements of the R_{xx} lower triangular part using equation (II.62)
Step 3:	Form the Toeplitz matrix T_{va} defined in equation (II.63)
Step 4:	Apply the EVD on T_{va} to define the signal subspace V_{1S} and the noise subspace V_{1N}
Step 5:	Define new min-norm vector u_{11} from the noise subspace V_{1N}
Step 6:	Estimate the DoAs of coherent signals by using the AT-MN spectrum expression according to equation (II.65)

II.7.2.2 Combined Cross-Correlation-Toeplitz MIN-NORM Algorithm

In this subsection, we introduce a second innovative method for estimating the Directions of Arrival (DoAs) of both coherent and non-coherent signals by utilizing a different

structure of the Toeplitz spatial covariance matrix. The concept involves adapting the Min-Norm DoA algorithm to operate with a reconstructed Toeplitz matrix rather than the traditional spatial covariance matrix. This reconstructed matrix is derived from an effective decorrelation technique known as the Cross-Correlation Vectors Toeplitz (CVT) method. Consequently, we have designated our second proposed method as CVT-Min-Norm[11]. It is important to note that the $M \times 1$ received signal vector $x(t)$ can be expressed as follows:

$$x(t) = [x_1(t), x_2(t), \ldots, x_M(t)] \tag{II.66}$$

Utilizing the CVT decorrelation technique as described , we calculate the received cross-correlation vector v_c. This vector is derived from the cross-correlation between the initial element of $x(t)$, which corresponds to the output of the first array sensor, and every element of the received signal vector that signifies the output from each sensor. Consequently, the components of the received cross-correlation vector v_c can be expressed as[11]:

$$v_c(i) = x_1(t)x_i^H(t), \quad i = 1, 2, \ldots, M \tag{II.67}$$

and the received cross-correlation vector is given as:

$$v_c = [v_c(1), v_c(2), \ldots, v_c(M)] \tag{II.68}$$

Now, we use the vector expressed in (II.76) to generate the following constructed Toeplitz matrix:

$$T_{vc} = \begin{bmatrix} v_c(1) & v_c(2) & \cdots & v_c(M) \\ v_c(2) & v_c(1) & \cdots & v_c(M-1) \\ \vdots & \vdots & \ddots & \vdots \\ v_c(M) & v_c(M-1) & \cdots & v_c(1) \end{bmatrix} \tag{II.69}$$

Reconstructing a Toeplitz matrix T_{vc} from the initial row of R_{xx} provides accurate Direction of Arrival (DoA) information. Specifically, the row space of the new matrix aligns perfectly with that of the ideal covariance matrix. The CVT decorrelation technique extracts DoA information without any interaction among sources, thereby ensuring robust decorrelation for coherent signals. The advancement of a new version of the Min-Norm algorithm, based on the Eigenvalue Decomposition (EVD) of this decorrelated Toeplitz matrix, will facilitate efficient DoA estimation for coherent sources[11].
The EVD of T_{vc} can be then expressed as

$$T_{vc} = \sum_{i=1}^{M} \omega_{2i} e_{2i} e_{2i}^H = V_{2S}\Omega_{2S}V_{2S}^H + V_{2N}\Omega_{2N}V_{2N}^H \tag{II.70}$$

where V_{2S} and V_{2N} are the signal and noise subspaces obtained thanks to the last matrix eigenvalue decomposition.

The CVT-Min-Norm spatial-spectrum can be formulated as

$$P_{\text{CVT-MN}}(\theta) = \frac{1}{\left|a^H(\theta)V_{2N}V_{2N}^H u_{21}\right|^2} \tag{II.71}$$

where u_{21} is the minimum norm vector belonging to the noise subspace V_{2N}.
The expression (II.71) is used to plot the CVT-Min-Norm spectrum. The locations of the peaks on CVT-Min-Norm spectrum indicate the correct DoAs of the incident signals. Thereupon, we can summarise this second proposition in the steps of Algorithm 2.

Algorithm 2: CVT-MN for estimating DOA of coherent signals

Step 1:	Estimates the autocorrelation matrix of receiving signals using equation (II.5)
Step 2:	Computes the received cross-correlation vectorv_c via equation(II.76)
Step 3:	Constructs the Toeplitz matrix T_{vc} defined in equation (II.77)
Step 4:	Generates the EVD of T_{vc} to determinate the signal subspaceV_{2S} and the noise subspace V_{2N}
Step 5:	Define new min-norm vector u_{21} from the noise subspace V_{2N}
Step 6:	Estimate the DOAs of coherent signals by employing the CVT-MN spectrum expression via equation (II.71)

II.7.2.3 Combined Averaging-Toeplitz MUSIC algorithm

In theory, and within specific limitations, the Min-Norm algorithm is capable of achieving high resolution in the estimation of arrival directions. However, its shortcomings are evident when estimating signals with low signal-to-noise ratios (SNR) or when dealing with highly correlated or coherent signal sources. To address these challenges, this subsection introduces and elaborates on a novel algorithm that relies on a transformation of the estimated Toeplitz spatial covariance matrix. We have developed an initial MUSIC DoA scheme utilizing a decorrelation technique. This technique involves averaging to create the components of a Toeplitz matrix. The algorithm introduced in this context is referred to as the Averaging Toeplitz for MUSIC (AT-MUSIC).
The last new Toeplitz matrix T_{va} (II.63) is mainly reconstituted from the averages of diagonals of coherent array covariance matrixR_{xx} . Thus, the superdiagonal entries of the reconstructed matrix T_{va} are a mixture of independent DoA terms and biased terms. This means that every column or row has one entry containing biased terms which leads to resolve the coherence signals problem, but it can result lower accuracy in the DoA estimation.
Currently, we utilize the decorrelated Toeplitz matrix T_{va} in place of the covariance matrix R_{xx} for the min-norm algorithm to determine the DoA. The matrix T_{va} can still be

characterized by its eigenvalues and eigenvectors as follows:

$$T_{va} = \sum_{i=1}^{M} \omega_{1i} e_{1i} e_{1i}^{H} = V_{1S} \Omega_{1S} V_{1S}^{H} + V_{1N} \Omega_{1N} V_{1N}^{H} \tag{II.72}$$

where V_{1S} and V_{1N}^{H} are the new signal and noise subspaces, respectively.
The derivation of the updated MUSIC spectrum expression relies on the computation of a novel MUSIC vector u_{11} that resides within the noise subspace V_{1N}, which is obtained from the decomposition of the Toeplitz matrix. Consequently, this spectrum is constructed as follows.

$$P_{\text{AT-MUSIC}}(\theta) = \frac{1}{a^{H}(\theta) V_n V_n^{H} a(\theta)} \tag{II.73}$$

The AT-MN algorithm is categorized as a spectral-based method. The function outlined in equation (II.73) can be utilized to generate the AT-MN spectrum, with the positions of the distinct highest peaks serving as the estimated DoAs

II.7.2.4 Combined Cross-Correlation-Toeplitz MUSIC Algorithm

In this subsection, we introduce a second innovative method for estimating the Directions of Arrival (DoAs) of both coherent and non-coherent signals by utilizing a different structure of the Toeplitz spatial covariance matrix. The concept involves adapting the MUSIC DoA algorithm to operate with a reconstructed Toeplitz matrix rather than the traditional spatial covariance matrix. This reconstructed matrix is derived from an effective decorrelation technique known as the Cross-Correlation Vectors Toeplitz (CVT) method. Consequently, we have designated our second proposed method as CVT-MUSIC It is important to note that the $M \times 1$ received signal vector $x(t)$ can be expressed as follows

$$x(t) = [x_1(t), x_2(t), \ldots, x_M(t)] \tag{II.74}$$

Utilizing the CVT decorrelation technique as described by Bai et al. (2010), we calculate the received cross-correlation vector v_c. This vector is derived from the cross-correlation between the initial element of $x(t)$, which corresponds to the output of the first array sensor, and every element of the received signal vector that signifies the output from each sensor. Consequently, the components of the received cross-correlation vector v_c can be expressed as

$$v_c(i) = x_1(t) x_i^{H}(t), \quad i = 1, 2, \ldots, M \tag{II.75}$$

and the received cross-correlation vector is given as

$$v_c = [v_c(1), v_c(2), \ldots, v_c(M)] \tag{II.76}$$

Now, we use the vector expressed in (II.76) to generate the following constructed Toeplitz matrix

$$T_{vc} = \begin{bmatrix} v_c(1) & v_c(2) & \cdots & v_c(M) \\ v_c(2) & v_c(1) & \cdots & v_c(M-1) \\ \vdots & \vdots & \ddots & \vdots \\ v_c(M) & v_c(M-1) & \cdots & v_c(1) \end{bmatrix} \tag{II.77}$$

Reconstructing a Toeplitz matrix T_{vc} from the initial row of R_{xx} provides accurate Direction of Arrival (DoA) information. Specifically, the row space of the new matrix aligns perfectly with that of the ideal covariance matrix. The CVT decorrelation technique extracts DoA information without any interaction among sources, thereby ensuring robust decorrelation for coherent signals. The advancement of a new version of the MUSIC algorithm, based on the Eigenvalue Decomposition (EVD) of this decorrelated Toeplitz matrix, will facilitate efficient DoA estimation for coherent sources.

The EVD of T_{vc} can be then expressed as

$$T_{vc} = \sum_{i=1}^{M} \omega_{2i} e_{2i} e_{2i}^H = V_{2S} \Omega_{2S} V_{2S}^H + V_{2N} \Omega_{2N} V_{2N}^H \tag{II.78}$$

where V_{2S} and V_{2N} are the signal and noise subspaces obtained thanks to the last matrix eigenvalue decomposition.

The CVT-MUSIC spatial-spectrum can be formulated as

$$P_{\text{CVT-MUSIC}}(\theta) = \frac{1}{|a^H(\theta) V_n V_n^H|^2} \tag{II.79}$$

where $a(\theta)$ is the array steering vector

The expression (II.79) is used to plot the CVT-MUSIC spectrum. The locations of the peaks on CVT-MUSIC spectrum indicate the correct DoAs of the incident signals.

II.8 Conclusion

This chapter presents a detailed overview of Direction of Arrival (DoA) estimation, covering signal modeling, the impact of signal coherence and correlation, and various estimation methods such as MUSIC, ESPRIT, CAPON, and MIN-NORM. It discusses the strengths and limitations of each technique, along with preprocessing methods like spatial smoothing and Toeplitz reconstruction to improve accuracy with coherent signals. The chapter concludes by highlighting the growing importance of integrating these techniques into real-time and intelligent systems for applications in communication, radar, sonar, and acoustic tracking.

Chapter III

Simulation results and discussion

III.1 Introduction

This chapter presents a comparative study of several DoA estimation algorithms, ranging from classical methods such as MUSIC and Min-Norm to the proposed techniques like AT-MN and AT-MUSIC, which rely on reconstructing the covariance matrix using the Toeplitz-based decorrelation technique. A series of simulations were conducted in a MATLAB environment to evaluate the performance of these algorithms under various conditions, including a limited number of snapshots, changes in the number of sources, and varying angles of arrival.
The simulation results are analyzed based on specific criteria such as angular resolution accuracy, the ability to distinguish between closely spaced sources, and robustness in the presence of signal correlation. These results highlight the effectiveness of the proposed methods compared to conventional algorithms, demonstrating their potential in improving DoA estimation performance in complex signal environments.

III.2 Comparison of DoA Estimation Methods for Non-Coherent Sources

III.2.1 Spectral Method Comparison

This simulation demonstrates and compares the performance of four spectral Direction of Arrival (DoA) estimation algorithms: MUSIC, Capon (MVDR), Min-Norm, and Classical Beamforming. The scenario involves an 8-element Uniform Linear Array (ULA) with standard half-wavelength element spacing receiving signals from three distinct sources located at angles of -15°, 10°, and 45°. These sources have differing powers (1.0, 1.5, and 1.2, respectively) and transmit uncorrelated, BPSK-like signals. The array operates in an environment corrupted by complex Additive White Gaussian Noise (AWGN) with a variance of 0.015. A defining characteristic of this simulation is the severely limited amount

of data used for estimation, with only K= 6 snapshots employed to compute the sample covariance matrix, thus testing the algorithms' capabilities under data-starved conditions.

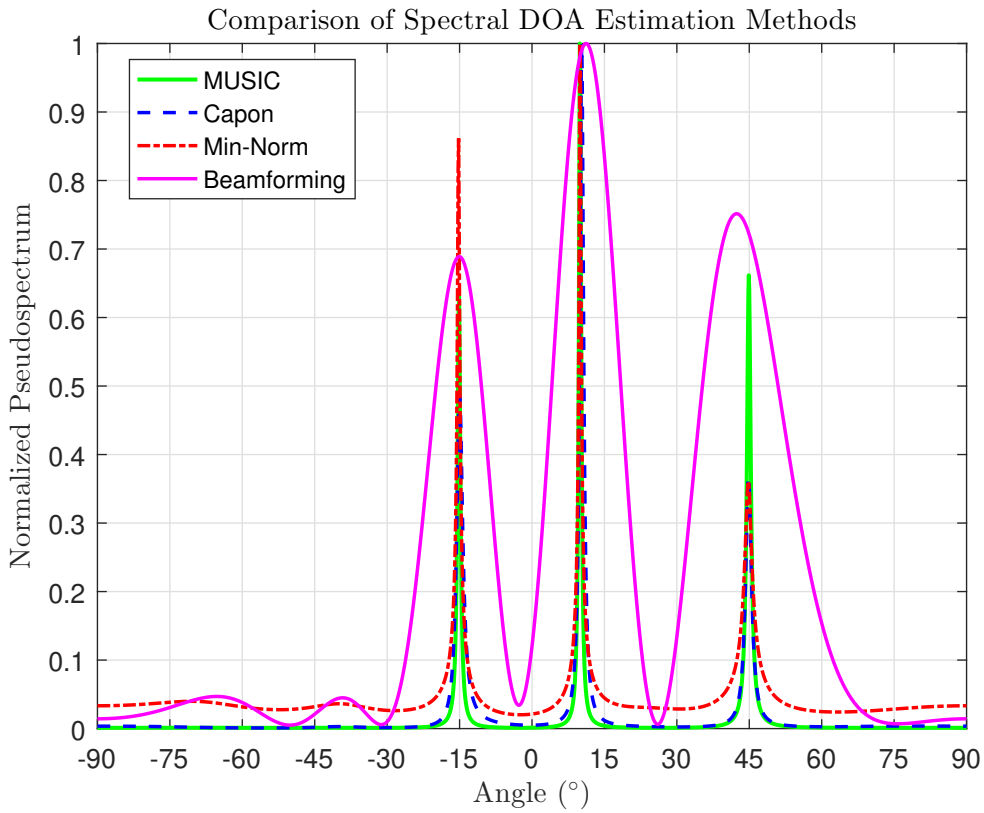

Figure III.1: DOA Estimation for Non-Coherent Sources

Figure III.1 illustrates the performance of four Direction of Arrival (DoA) estimation techniques: MUSIC, Capon, Min-Norm, and Conventional Beamforming, based on their normalized pseudospectra as a function of angle. The x-axis represents the angle in degrees, while the y-axis displays the normalized pseudospectrum, indicating the likelihood of signal presence from a given direction. The MUSIC algorithm (solid green line) provides the sharpest and most distinct peaks at the actual source angles, reflecting its high resolution and effectiveness in resolving closely spaced signals. The Capon method (solid blue line) also exhibits relatively sharp peaks, albeit with slightly lower resolution than MUSIC. Min-Norm (red dashed line) shows performance comparable to that of MUSIC and Capon, but with somewhat reduced peak prominence. Conventional Beamforming (magenta line) displays broad and less defined peaks, resulting in poor angular resolution and potential difficulty in distinguishing sources with minimal angular separation. Overall, this spectral comparison highlights the superior resolution capabilities of MUSIC, particularly in scenarios involving closely spaced incoming signals.

III.2.1.1 Comparison between MUSIC and ESPRIT

This simulation example investigates Direction of Arrival (DoA) estimation by comparing the MUSIC and ESPRIT algorithms. The scenario involves three uncorrelated, narrowband signal sources arriving at angles of -25°, -20° (representing a closely spaced pair), and 30° onto an 8-element Uniform Linear Array (ULA) with standard half-wavelength spacing. The signals, each with unit average power, are embedded in spatially and temporally white complex Gaussian noise, resulting in a Signal-to-Noise Ratio (SNR) of 15 dB per source. DOA estimates are derived from 200 snapshots of received data using both the subspace-based search method of MUSIC and the rotational invariance technique of ESPRIT.

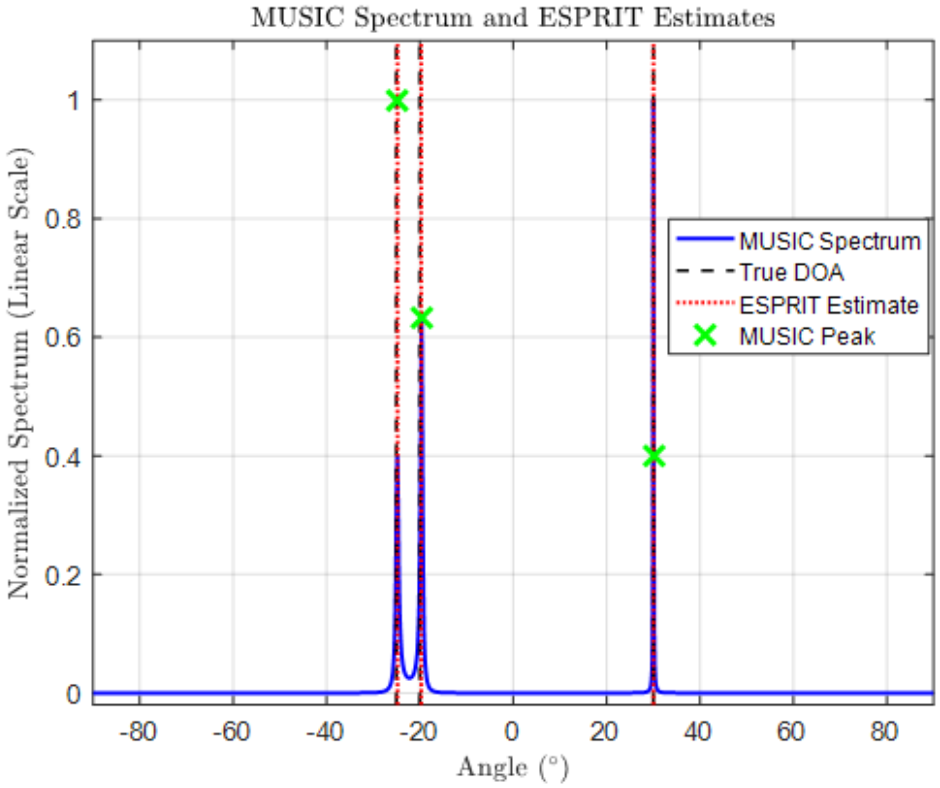

Figure III.2: MUSIC Spectrum and ESPRIT Estimation

This figure presents a comparison of the direction of arrival (DoA) estimation results obtained through the MUSIC and ESPRIT methods, juxtaposed with the actual source directions (True DoA). The blue curve illustrates the MUSIC spectrum, normalized and displayed on a linear scale, revealing three prominent peaks that signify the DOA estimates provided by MUSIC. The dashed black lines represent the actual DOA of the sources. The dashed red lines indicate the estimates derived from ESPRIT, which appear to align very closely with the true DOA. The green crosses (MUSIC Peak) denote the maximum values of the MUSIC spectrum, corresponding to the estimated directions

by this method. The graph demonstrates that both MUSIC and ESPRIT successfully estimate the directions of arrival with high accuracy, closely matching the true directions. However, it is important to note that MUSIC requires spectral searching (angular scanning), while ESPRIT directly provides the angles without the need for a spectrum, making ESPRIT faster but reliant on stricter assumptions, such as the uniform structure of the antenna.

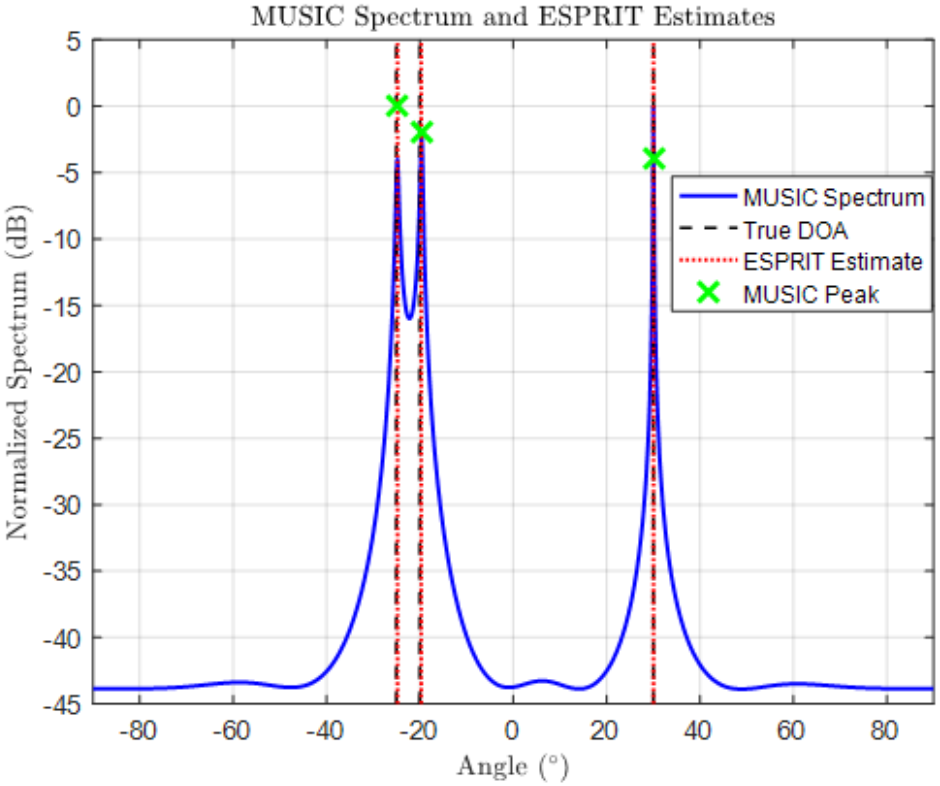

Figure III.3: MUSIC Spectrum and ESPRIT Estimation

This diagram depicts a comparison of the performance between the MUSIC algorithm and the ESPRIT method in estimating direction-of-arrival (DOA). The MUSIC spectrum, displayed on a logarithmic scale (in dB), reveals three distinct and sharp peaks (indicated by green crosses), which align with the estimated directions. These peaks are in close proximity to the actual DoAs (represented by dotted black lines) and the ESPRIT estimates (shown by dotted red lines), demonstrating the high accuracy of both techniques. The logarithmic scale emphasizes MUSIC's capability to effectively differentiate between closely situated sources, even amidst noise. Conversely, ESPRIT delivers estimates without the need for angular scanning, significantly lowering computational complexity while achieving accuracy that is comparable to that of MUSIC. Therefore, it can be concluded that: MUSIC provides superior angular resolution and excels in scenarios involving closely spaced sources. Although ESPRIT may exhibit slightly reduced resolution under specific conditions, it serves as a rapid and efficient alternative, particularly when computational time is of the essence.

III.2.1.2 RMSE-Based Comparison of DoA Estimation Techniques over Varying SNR Levels

This simulation aims to evaluate and compare the performance of four prominent Direction of Arrival (DoA) estimation algorithms—MUSIC, Capon (MVDR), Min-Norm, and conventional Beamforming—under varying noise conditions. The scenario involves two narrowband signal sources impinging on a Uniform Linear Array (ULA) consisting of 8 antenna elements, spaced at half the signal wavelength (0.5). To simulate realistic conditions, 50 temporal snapshots are used per trial, and results are averaged over 200 Monte Carlo runs to ensure statistical reliability. The Signal-to-Noise Ratio (SNR) is swept from −5 dB to 25 dB to observe its effect on estimation accuracy. For each SNR level, the Root Mean Square Error (RMSE) of the estimated angles is computed, serving as the performance metric. The resulting RMSE curves provide a clear comparison of the robustness and resolution capabilities of the tested algorithms, highlighting their respective strengths and limitations across different noise environments.

The simulation results highlight that MUSIC and Capon/MVDR consistently outper-

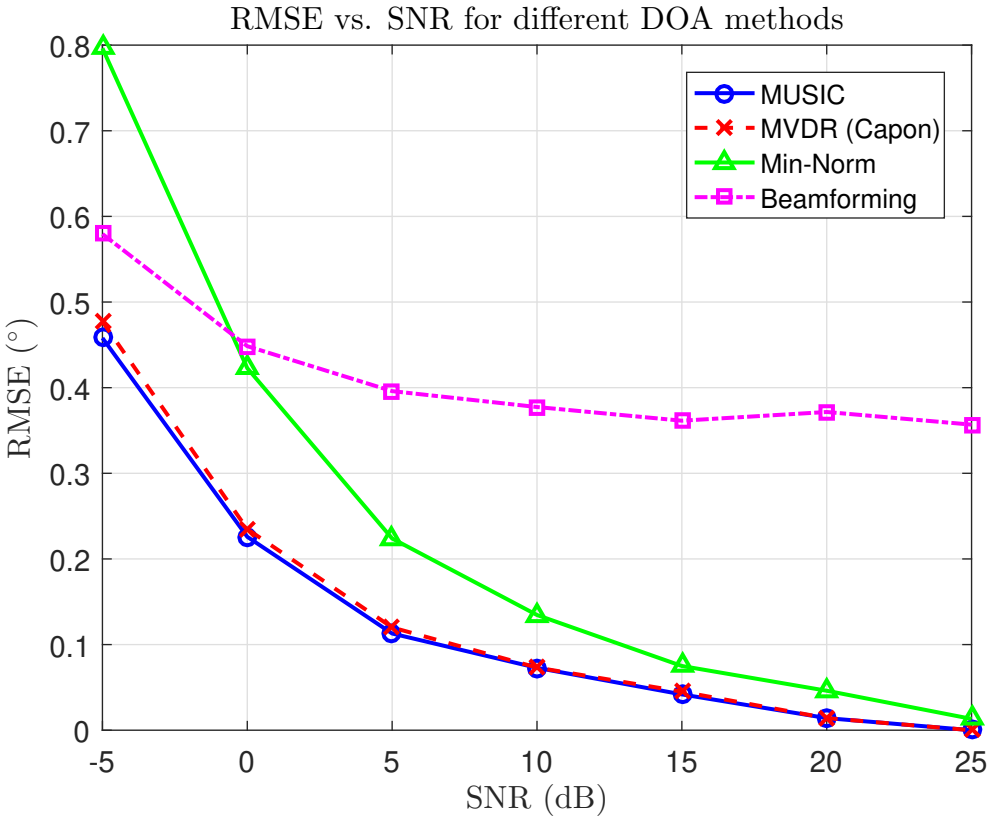

Figure III.4: DOA Estimation RMSE

form Min-Norm and Beamforming across all SNR levels. MUSIC achieves the lowest RMSE, particularly at higher SNRs, leveraging the orthogonality between signal and noise subspaces for precise estimation. Capon/MVDR follows closely, benefiting from its adaptive beamforming, although its RMSE is slightly higher at high SNRs. Min-Norm

suffers from noise sensitivity at low SNR but improves with increasing SNR, eventually approaching MUSIC's performance in ideal conditions. Beamforming performs the worst, with a nearly constant RMSE, illustrating its limitations in resolution and noise resilience. These results emphasize the effectiveness of subspace-based methods (MUSIC, Capon) in practical DOA estimation tasks, with MUSIC being computationally demanding but ideal for applications where accuracy is crucial.

III.3 DoA Estimation Methods for Coherent Sources

III.3.1 Method Based on Toeplitz Matrix Reconstruction

This simulation example demonstrates and compares the estimation of direction of arrival (DoA) using the MUSIC algorithm under challenging conditions with coherent signal sources. The scenario involves two coherent signals (generated using identical frequencies and a fixed amplitude/phase relationship) arriving at -20° and 10° onto a 8-element Uniform Linear Array (ULA) with standard half-wavelength spacing. Data is collected over 500 snapshots in the presence of Additive White Gaussian Noise, resulting in a Signal-to-Noise Ratio (SNR) of 10 dB. Since standard MUSIC fails with coherent sources due to the rank deficiency of the sample covariance matrix, the example implements and compares two common decorrelation techniques: CTOP (Correlation Toeplitz, reconstructed from the first row of covariance matrix and made Hermitian) and AVTOP (Averaged Diagonals Toeplitz, reconstructed from the averaged diagonals of covariance matrix and made Hermitian). MUSIC is applied separately using the noise subspaces derived from the standard covariance matrix, the CTOP matrix, and the AVTOP matrix. The resulting normalized pseudospectra are plotted on a single graph to visually assess the ability of CTOP and AVTOP preprocessing to restore MUSIC's capability to resolve coherent sources compared to the standard MUSIC.
The illustration (III.5) contrasts the spectral capabilities of three variations of the MUSIC algorithm utilized for direction-of-arrival (DOA) estimation: standard MUSIC (depicted in black), AVTOP MUSIC (shown in red), and CTOP MUSIC (represented in blue). This is presented in a logarithmic scale (in dB) of the spatial spectrum relative to angle. AVTOP MUSIC exhibits distinct, sharply defined peaks at the angles corresponding to the actual sources, signifying exceptional resolution and accurate detection even amidst noise. Although CTOP MUSIC presents broader peaks compared to AVTOP, it still outperforms standard MUSIC regarding angular resolution. In contrast, standard MUSIC reveals a broader spectrum with more pronounced side lobes and considerably diminished angular resolution. This analysis underscores the advantages of the AVTOP and CTOP modifications over the traditional MUSIC algorithm. Notably, AVTOP MUSIC achieves optimal angular resolution, rendering it ideal for environments characterized by significant interference or closely situated sources.

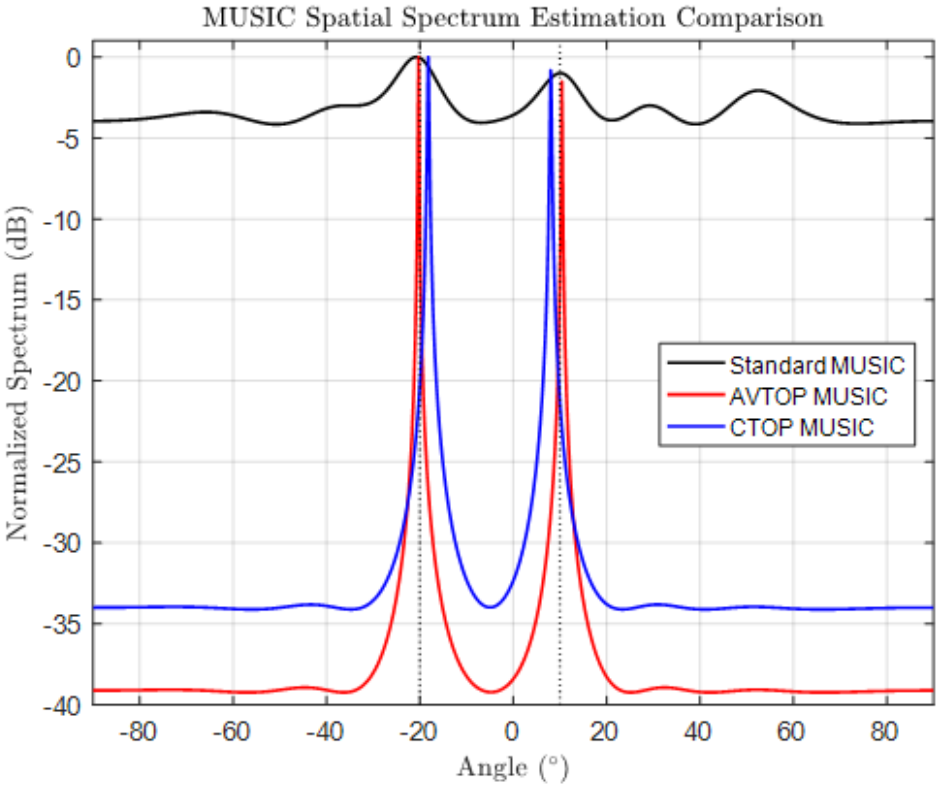

Figure III.5: MUCIC Spatial Estimation Comparison

CTOP MUSIC strikes a balance between performance and robustness, making it advantageous for less intricate scenarios. Conversely, standard MUSIC, while straightforward, is constrained in its effectiveness under complex conditions.

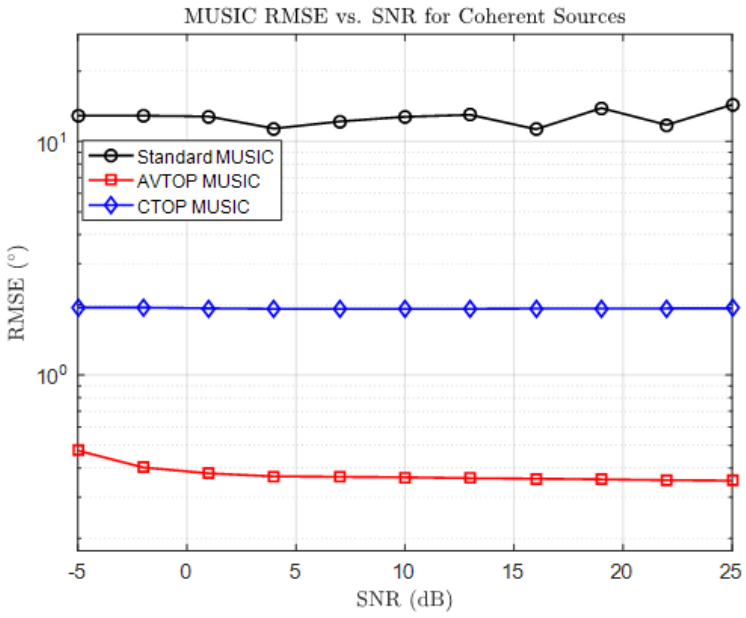

Figure III.6: MUSIC RMSE vs. SNR for Coherent Sources

This simulation (III.6) assesses the performance of the Root Mean Square Error (RMSE) for three variants of the MUSIC algorithm—Standard MUSIC, CTOP-MUSIC, and AVTOP-MUSIC—in estimating the Direction of Arrival (DOA) of two fully coherent sources located at $-20°$ and $10°$. The evaluation utilizes an 8-element Uniform Linear Array (ULA) with /2 spacing. The coherence of the signals leads to a rank-deficient covariance matrix, which adversely affects the performance of standard MUSIC. In contrast, CTOP-MUSIC and AVTOP-MUSIC mitigate this issue by reconstructing a Hermitian Toeplitz matrix—CTOP-MUSIC does so from the first row, while AVTOP-MUSIC employs an averaging method across the matrix diagonals. The RMSE is calculated over 200 Monte Carlo trials, each consisting of 500 snapshots, across signal-to-noise ratios (SNRs) ranging from -5 dB to 25 dB. The findings indicate that both CTOP and AVTOP outperform standard MUSIC, with AVTOP demonstrating the highest overall accuracy.
This illustration contrasts the efficacy of three variations of the MUSIC algorithm—Standard MUSIC, AVTOP MUSIC, and CTOP MUSIC—regarding the root-mean-square error (RMSE) in direction-of-arrival (DoA) estimation, as influenced by the signal-to-noise ratio (SNR) for coherent sources. The findings distinctly highlight the superiority of AVTOP MUSIC (represented by the red curve), which consistently exhibits lower RMSE values compared to the other two methods across the entire tested SNR spectrum. This enhancement indicates remarkable resolution capabilities and increased resilience against noise and source coherence. The CTOP MUSIC approach (depicted by the blue curve) maintains a relatively stable RMSE of approximately $2°$, positioning it above AVTOP but significantly below the standard method, thus serving as a viable balance between complexity and performance. Conversely, the standard MUSIC method (illustrated by the black curve) demonstrates the least effective performance, characterized by a high RMSE and minimal responsiveness to SNR improvements, indicating low efficiency in scenarios involving coherent sources.

III.3.2 Spatial Smoothing Methods

III.3.2.1 Forward Smoothing with Min-Norm

This simulation illustrates the performance of the Min-Norm algorithm in estimating the Direction of Arrival (DOA) under the presence of coherent sources using forward spatial smoothing. The experiment assumes two coherent narrowband signals impinging at incident angles of approximately $-10°$ and $5°$ on an 8-element Uniform Linear Array (ULA) with half-wavelength inter-element spacing. Due to the coherence between the sources and the limited number of temporal snapshots, traditional subspace-based methods struggle to resolve the sources accurately. To address this, forward spatial smoothing is applied to the sample covariance matrix to restore rank and enable subspace separation. The resulting smoothed covariance matrix is used to compute the noise subspace via Singular Value Decomposition (SVD), and the Min-Norm pseudospectrum is generated

over the angular range from −90° to 90°. The plot shows distinct spectral peaks at the true angles of arrival, confirming the algorithm's effectiveness in resolving closely spaced coherent sources when aided by forward smoothing. The spectrum is plotted in decibels to emphasize the dynamic range and peak sharpness, providing clear visual evidence of DOA estimation accuracy.

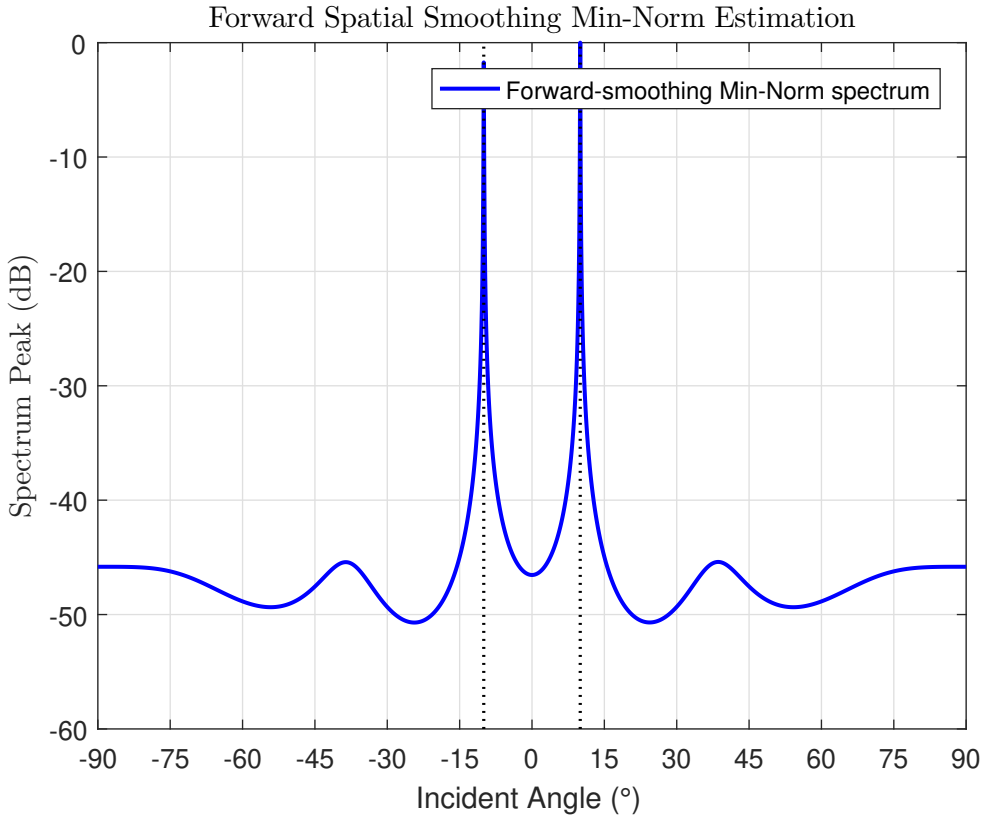

Figure III.7: Forward Spatial Smoothing Min-Norm Estimation

The illustration presents the outcomes of the Min-Norm algorithm utilized in conjunction with the Forward Spatial Smoothing technique for the estimation of angles of arrival (DOA) of coherent sources. The spectrum reveals two distinct, sharply defined peaks situated at angular positions that align with the directions of the incoming sources, underscoring the method's exceptional angular precision. The remarkably low sidelobe levels (below -50 dB) indicate the enhanced resolution of this technique, as well as its resilience in the presence of correlated sources or noise. Spatial smoothing disrupts the coherence among sources and enhances the quality of the covariance matrix, which is essential for effective estimation using the Min-Norm method.

III.3.2.2 Backward Smoothing with Min-Norm

This simulation analyzes the efficacy of the Min-Norm algorithm for Direction of Arrival (DOA) estimation, employing backward spatial smoothing to address two coherent sources located at 32° and 43°. The signals are captured by an 8-element Uniform Linear

Array with a spacing of 0.5 . The coherence of the signals results in a rank-deficient covariance matrix, which poses challenges for traditional subspace methods. However, backward smoothing mitigates this issue by creating a smoothed covariance matrix from reversed subarrays. Through Singular Value Decomposition (SVD), the noise subspace is identified, and the Min-Norm pseudospectrum is calculated over the range of $-90°$ to $90°$. The resulting spectrum exhibits distinct peaks at the actual DOAs, thereby illustrating the effectiveness of backward smoothing in distinguishing coherent signals.

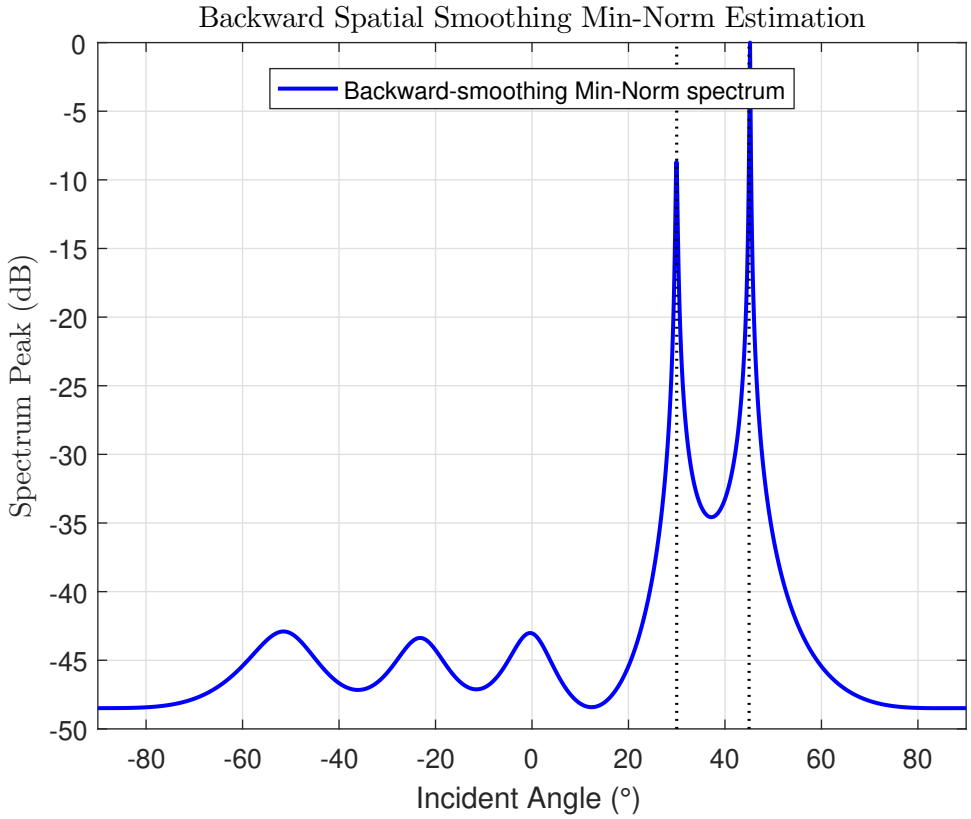

Figure III.8: Backward Spatial Smoothing Min-Norm Estimation

The figure demonstrates the performance of the Min-Norm method with Backward Spatial Smoothing for estimating Direction of Arrival (DOA) angles. Two distinct spectral peaks are observed around $30°$ and $45°$, indicating that the method successfully identifies the presence of two incident sources within this angular range. Compared to the version utilizing Forward Spatial Smoothing, the spectral structure here exhibits higher side lobes (approximately -40 dB), which may potentially limit resolution capabilities in complex scenarios. Nevertheless, the accuracy of angle detection remains satisfactory, and this technique presents a viable alternative, particularly when the rear symmetry of the antenna can be leveraged to enhance covariance matrix estimation. This type of smoothing is beneficial in certain antenna configurations or when signals exhibit a specific spatial structure (e.g., back-propagated signals). It can also be combined with forward smoothing to create a bidirectional smoothing approach, thereby maximizing resilience

to inter-source coherence.

III.3.2.3 Bidirectional Smoothing with Min-Norm

This simulation estimates the Directions of Arrival (DOAs) for two coherent signals, arriving at 5 and 10 degrees onto an 8-element uniform linear array. The simulation uses 1024 time samples (snapshots) and operates at a Signal-to-Noise Ratio (SNR) of 10 dB. The antenna elements are spaced at half the wavelength. Because standard subspace DOA methods perform poorly with coherent sources, this simulation example first applies Forward-Backward Spatial Smoothing which divides the 8-element array into smaller overlapping 6-element subarrays (3 forward, 3 backward). By averaging the covariance matrices of these subarrays, the coherence between the signals is effectively broken, restoring the rank of the signal covariance matrix. Subsequently, the high-resolution Min-Norm algorithm is used on this smoothed covariance matrix to compute a spatial spectrum, aiming to reveal sharp peaks at or very near the true signal angles, thereby demonstrating the effectiveness of the combined Forward-Backward Smoothing and Min-Norm technique for resolving coherent sources.

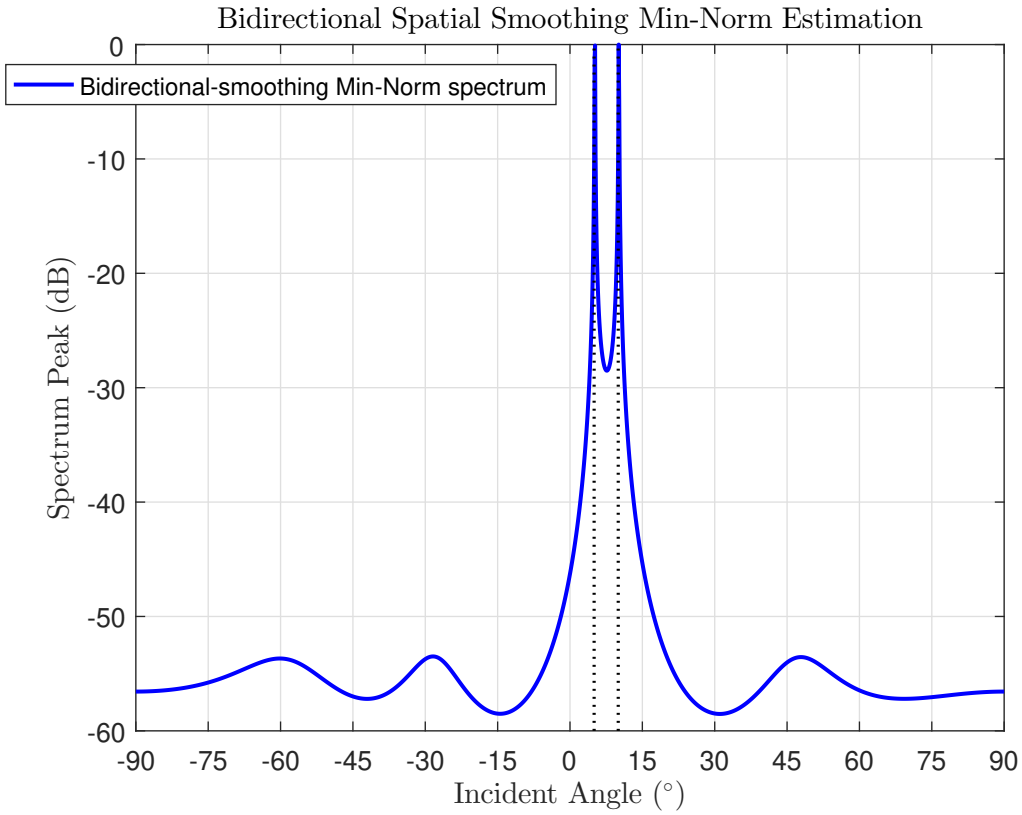

Figure III.9: Bidirectional Spatial Smoothing Min-Norm Estimation

This plot illustrates the bidirectional spatial smoothing Min-Norm spectrum for direction-of-arrival (DOA) estimation. The spectrum displays two prominent and well-resolved

peaks near 0° and 10°, corresponding to the actual incident angles of the sources. The clear separation between these peaks demonstrates the method's ability to resolve closely spaced sources, even under challenging conditions such as limited snapshots or coherent sources. The presence of moderate side lobes suggests some residual spectral leakage, which is a known limitation of the Min-Norm method, particularly under noisy conditions. Nonetheless, the overall peak sharpness and low noise floor indicate that bidirectional spatial smoothing effectively enhances resolution and mitigates the impact of source coherence. This result confirms the potential of Min-Norm with spatial smoothing as a viable subspace-based approach for DOA estimation

III.4 MIN NORM DoA Estimation under Snapshot Limitations

This simulation assesses the efficacy of the Min-Norm algorithm for Direction of Arrival (DOA) estimation in challenging scenarios characterized by coherent sources and severely limited data. Two coherent narrowband signals, which share the same angular frequency and maintain a fixed phase relationship, are received from angles of 0° and 10° at a Uniform Linear Array (ULA) consisting of 8 elements spaced at half-wavelength intervals (0.5). The estimation of the covariance matrix is based on only 6 snapshots, indicative of a data-sparse environment. The array operates under complex Additive White Gaussian Noise (AWGN) conditions with a Signal-to-Noise Ratio (SNR) of 10 dB. To address the challenges posed by source coherence and rank deficiency, the simulation employs spatial smoothing techniques—forward (Rf), backward (Rb), and forward-backward (Rbf). For each scenario, the Min-Norm spectrum is calculated using the noise subspace derived from Singular Value Decomposition (SVD) and is plotted over the angular range from $-90°$ to 90°. The resulting pseudospectra facilitate a visual comparison of the various smoothing methods. As anticipated, the forward-backward smoothing (Rbf) technique produces the most distinct peaks at the actual DOAs, highlighting its capability to effectively resolve coherent sources even with limited data.

The Min-Norm Spectrum Figure Analysis: This figure illustrates the effectiveness of different spatial smoothing techniques—Forward only (Rf), Backward only (Rb), and Forward-Backward (Rbf)—in ascertaining the Direction of Arrival (DoA) using the Min-Norm algorithm. The horizontal axis represents the incident angle in degrees, while the vertical axis reflects the spectrum peak in dB. The Forward-Backward method (depicted by the blue line) produces the most accurate and distinct peaks, successfully identifying incoming signal directions around $\pm 10°$. This establishes it as the most effective method for differentiating closely spaced signals.

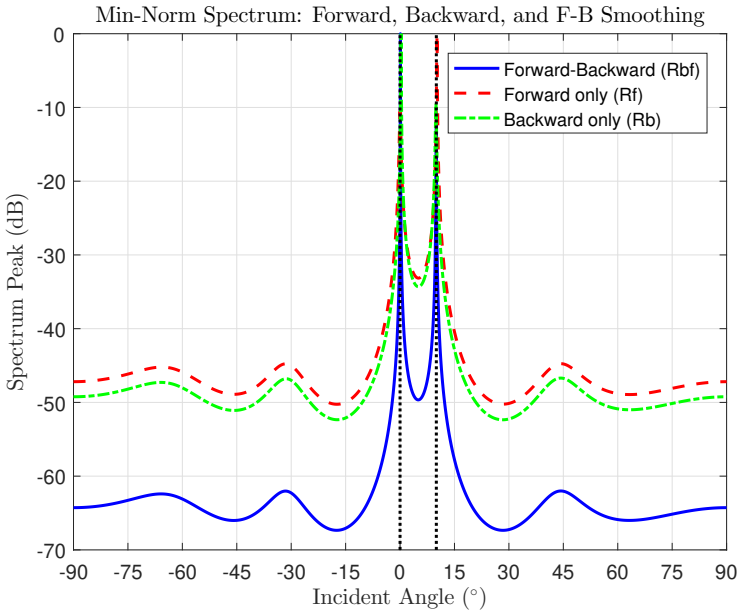

Figure III.10: Min-Norm Spectrum: Forward, Backward, and F-B Smoothing

In contrast, the Forward only (represented by the red dashed line) and Backward only (shown by the green dashed line) methods generate broader peaks with reduced resolution, particularly the backward-only method, which demonstrates inferior performance. This evaluation highlights the importance of utilizing Forward-Backward smoothing to improve DoA estimation in adaptive antenna systems. The results clearly demonstrate that the Forward-Backward smoothing technique is the most efficient among the three methods, as it provides enhanced angular discrimination and the capability to handle interrelated sources, making it the optimal choice for intelligent systems that depend on antenna arrays in intricate environments.

III.5 DoA Estimation for Coherent Sources using Min-Norm with Spatial Smoothing

This simulation assesses the efficacy of the Min-Norm algorithm combined with spatial smoothing for estimating the Direction of Arrival (DoA) amidst coherent sources. A Uniform Linear Array (ULA) consisting of 10 elements, spaced half a wavelength apart, captures signals from three coherent sources positioned at angles of -20°, -10°, and 20°. The coherence among the sources can lead to the failure of conventional techniques such as MUSIC due to the deficiency in the covariance matrix rank. To mitigate this issue, forward-backward spatial smoothing is employed, which restores the rank and facilitates accurate estimation. Operating under a signal-to-noise ratio (SNR) of 10 dB with 100 snapshots, the smoothed covariance matrix is utilized in the Min-Norm algorithm to determine DOAs by locating polynomial roots in proximity to the unit circle. The outcomes

are depicted through:

1. A Spectral Min-Norm Plot that illustrates the normalized power spectrum alongside the estimated and true DoAs.

2. A Root Distribution Plot on the complex plane displaying all roots and selected roots.

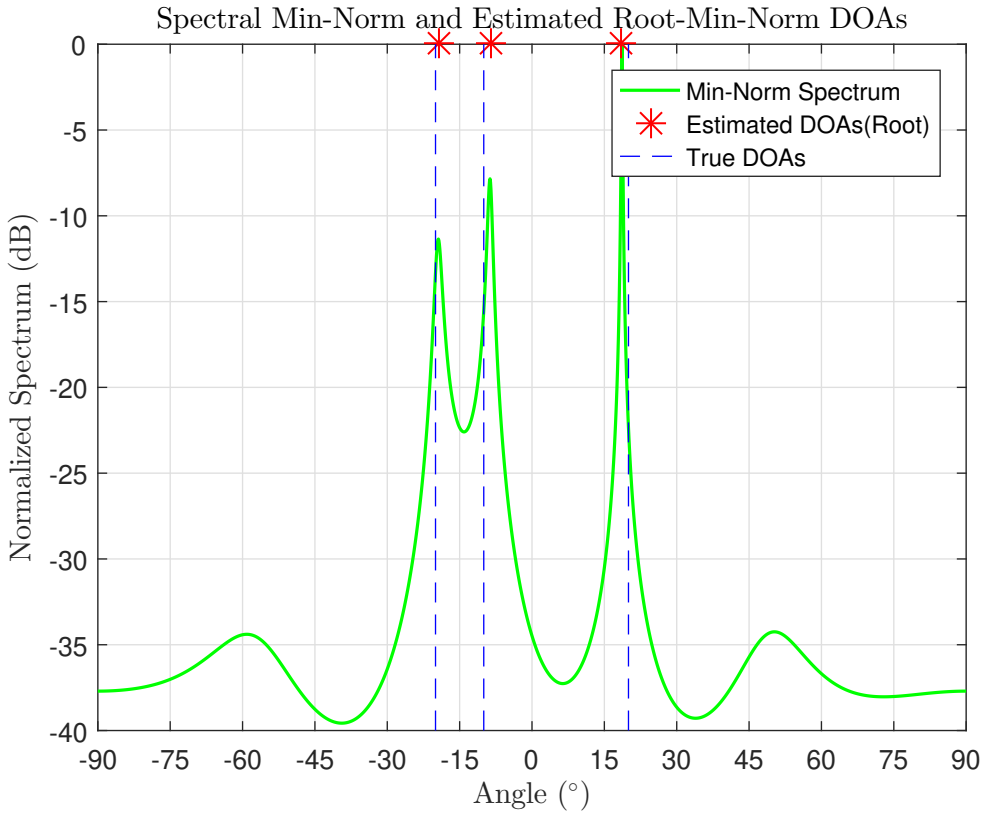

Figure III.11: Spectral Min-Norm and Estimated Root-Min-Norm DOAs

This illustration showcases the effectiveness of the Root-Min-Norm algorithm in estimating the Directions of Arrival (DOAs) for multiple coherent sources. The first graph presents the roots of the polynomial derived from the Min-Norm spectrum within the complex plane. A dashed line outlines the unit circle, serving as a reference to identify significant roots. The blue crosses denote all computed roots, while the red circles highlight the selected roots that are closest to the unit circle—these roots correspond to the estimated DOAs. Their proximity to the unit circle is a crucial indicator of their importance in determining signal directions, as per the Root-Min-Norm methodology.
The subsequent figure illustrates the spectral outcomes of the Min-Norm algorithm, alongside the estimated and actual DOAs. The green curve represents the normalized Min-Norm spectrum (in dB), displaying clear peaks at the expected signal directions. Red stars mark the peak positions identified from the spectrum, which correspond with the DOAs obtained through the root selection technique. The dashed blue lines indicate the

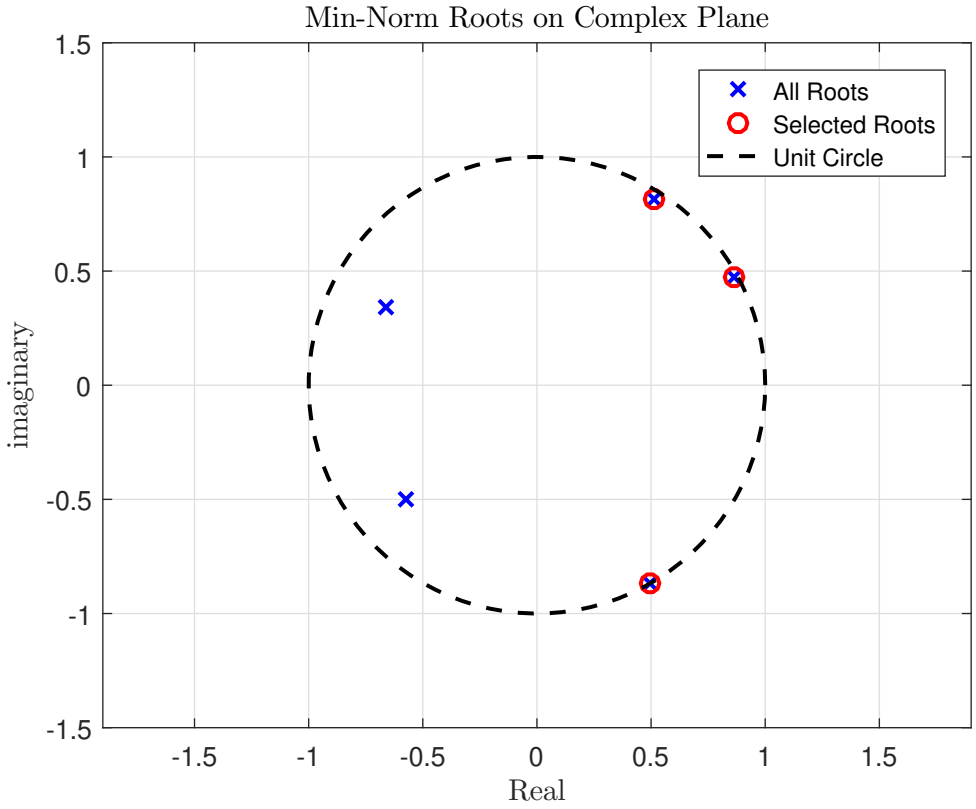

Figure III.12: Min-Norm Roots on Complex Plane

actual DOAs utilized in the simulation, reinforcing the algorithm's capability to accurately distinguish multiple closely spaced and coherent sources.
This visualization validates the effectiveness of the Root-Min-Norm approach in scenarios involving coherent sources, particularly when enhanced with spatial smoothing. Unlike traditional spectral methods such as MUSIC, which require an exhaustive angle search, the root-based technique allows for the direct computation of DOAs from polynomial roots. This not only improves efficiency but also maintains accuracy, provided that the array maintains a consistent and linear configuration.

III.6 DoA Estimation for Coherent Sources using MUSIC with Spatial Smoothing

This simulation assesses the efficacy of the MUSIC algorithm combined with spatial smoothing for estimating the Direction of Arrival (DoA) amidst coherent sources. A Uniform Linear Array (ULA) consisting of 10 elements, spaced half a wavelength apart, captures signals from three coherent sources positioned at angles of -20°, -10°, and 20°. The coherence among the sources can lead to the failure of conventional techniques such as due to the deficiency in the covariance matrix rank. To mitigate this issue, forward-backward spatial smoothing is employed, which restores the rank and facilitates accurate

estimation. Operating under a signal-to-noise ratio (SNR) of 10 dB with 100 snapshots, the smoothed covariance matrix is utilized in the Min-Norm algorithm to de- termine DOAs by locating polynomial roots in proximity to the unit circle. The outcomes are depicted through:

1. A Spectral MUSIC Plot that illustrates the normalized power spectrum alongside the estimated and true DoAs.

2. A Root Distribution Plot on the complex plane displaying all roots and selected roots.

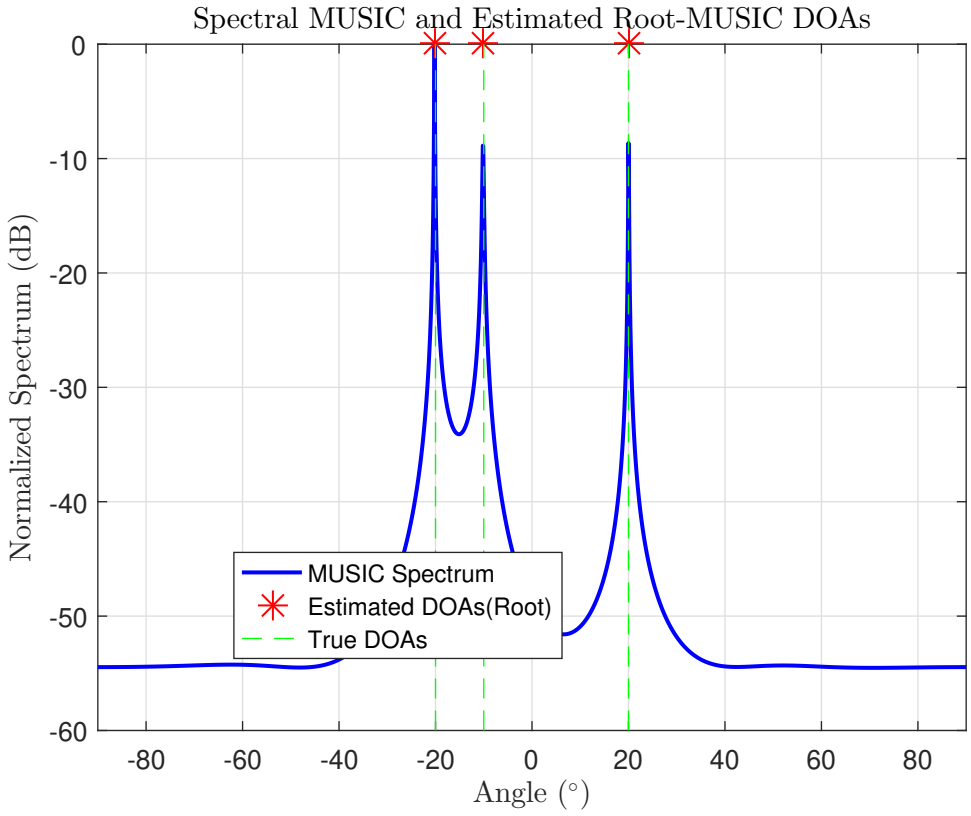

Figure III.13: Spectral MUSIC and Estimated Root-MUSIC DOAs

This plot illustrates the spectral pseudo-spectrum obtained using the MUSIC algorithm for direction-of-arrival (DOA) estimation. Two dominant peaks are observed near –20° and 15°, corresponding to the true incident angles of the sources. The Root-MUSIC estimated DOAs, marked by red asterisks, closely align with the true source directions (indicated by vertical dashed lines), confirming the high estimation accuracy of the method. The sharpness and narrow width of the spectral peaks reflect the high resolution capability of MUSIC, even under conditions of limited snapshots or source correlation. The presence of a low noise floor and minimal spectral leakage further validates the robustness of MUSIC as a subspace-based DOA estimation technique. This comparison also demonstrates the close agreement between the spectral and root-based variants of MUSIC in

practical scenarios.

This plot presents the distribution of polynomial roots obtained in the Root-MUSIC algorithm for direction-of-arrival (DOA) estimation. The unit circle is shown as a reference (dashed line), and all computed roots are marked with blue crosses. The roots selected for DOA estimation—those closest to the unit circle and located outside it—are highlighted with red circles. The clustering of selected roots near the unit circle confirms the theoretical foundation of Root-MUSIC, which exploits the orthogonality between the signal and noise subspaces. The angular positions of these roots directly correspond to the estimated source directions. This visual representation highlights the algorithm's ability to distinguish signal-related roots from noise-induced roots, especially under challenging estimation scenarios.

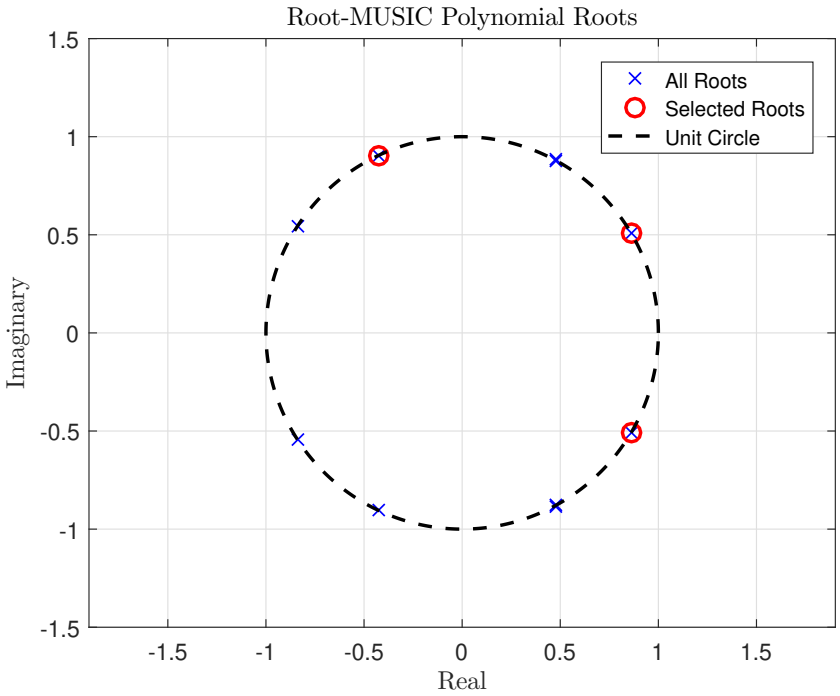

Figure III.14: Root Distribution in Root-MUSIC Algorithm

III.7 Conclusion

This chapter presents a detailed overview of Direction of Arrival (DoA) estimation, covering signal modeling, the impact of signal coherence and correlation, and various estimation methods such as MUSIC, ESPRIT, CAPON, and MIN-NORM. It discusses the strengths and limitations of each technique, along with preprocessing methods like spatial smoothing and Toeplitz reconstruction to improve accuracy with coherent signals. The chapter concludes by highlighting the growing importance of integrating these techniques into real-time and intelligent systems.

General Conclusion

This study offered an extensive examination of Direction of Arrival (DoA) estimation, outlining both the theoretical principles and practical difficulties encountered in signal processing within array systems. We began with the signal model, investigating the mathematical representation of signals received by an array and how critical parameters such as coherence and correlation among signals affect the effectiveness of DoA algorithms. Particular emphasis was placed on differentiating between coherent and non-coherent signals, as this significantly impacts the selection and precision of estimation methods. A broad spectrum of DoA estimation techniques was reviewed, including subspace-based algorithms like MUSIC, ROOT-MUSIC, and ESPRIT, as well as power spectrum and minimum norm approaches such as CAPON and MIN-NORM. Each method was analyzed regarding its underlying assumptions, benefits, and drawbacks. Acknowledging the challenges presented by signal correlation and coherence, we also examined effective strategies to alleviate their effects. Spatial smoothing was identified as a commonly utilized approach for managing coherent sources, while the Toeplitz method was highlighted as a useful technique for restoring the covariance matrix structure in cases of partial correlation loss. The integration of robust signal modeling, effective Direction of Arrival (DoA) estimation techniques, and pre-processing methods such as spatial smoothing and Toeplitz reconstruction facilitates dependable source localization, even in intricate signal environments. As array signal processing advances—propelled by its applications in wireless communication, radar, sonar, and acoustic tracking—the amalgamation of these techniques with real-time systems and intelligent processing frameworks will be crucial in enhancing the precision and adaptability of DoA estimation. This research further substantiates these findings through simulation results that demonstrate the performance of the analyzed algorithms across various operational scenarios. In situations with limited snapshots, subspace-based methods like MUSIC and ESPRIT showed high resolution and accuracy when the incoming signals were uncorrelated. However, their effectiveness significantly diminished in the presence of coherent sources. Techniques such as CAPON and MIN-NORM, while not as sharp in resolution, proved to be more resilient under these challenging circumstances. The use of forward-backward spatial smoothing greatly enhanced estimation accuracy for coherent signals, while Toeplitz matrix reconstruction successfully restored the covariance structure, thereby improving the overall stability of the algorithms. These results emphasize the necessity of merging theoretical insights with practical improvements to achieve reliable DoA estimation in real-world settings.

References

[1] H. Hafsi, *Étude des algorithmes performants pour la synthèse de diagramme de rayonnement des réseaux d'antennes*. Master académique, Université Kasdi Merbah Ouargla, 2020.

[2] Z. Bachir, "Modélisation d'une antenne micro ruban compacte," *Master académique, Université EchahidHamma Lakhdar-El oued*, 2015.

[3] A. Boyer, "support de cours énonce de travaux diriges," *Institut National des Sciences Appliquées de Toulouse 5ème Année Réseau et Télécom*, p. 79, 2011.

[4] A. Bakouche and M. Mekkaouche, "L'effet des caractéristiques de l'antenne patch sur sa directivité," *mémoire de master, Université de Béjaia*, 2014.

[5] N. Guellil, *Etude et conception d'un réseau d'antennes beamforming à base de la matrice de Butler en utilisant ADS Momentum*. PhD thesis, Université de Setif 1, 2018.

[6] N. J. G. Fonseca, *Etude de Systèmes Micro-ondes d'Alimentation d'Antennes Réseaux pour Applications Multifaisceaux*. PhD thesis, Institut National Polytechnique de Toulouse-INPT, 2010.

[7] A. Naceur and B. Merahi, "L'estimation de l'angle d'arrivée et la formation de voie par un système à antenne intelligente," in *International Congress on telecommunication and application (ICTA'12), Béjaia, Algeria*, 2012.

[8] N. Aounallah, *Utilisation des antennes intelligentes dans les systèmes de communications sans fil*. PhD thesis, Université de Sidi Bel Abbès-Djillali Liabes, 2015.

[9] N. Aounallah and M. Bouziani, "The use of high resolution algorithms for angle of arrival estimation," in *ICMIP'12, Mascara, Algeria*, 2012.

[10] K. Atteya and M. Amer, "Indoor positioning—bluetooth angle of arrival," *Lund University*, 2019.

[11] N. Aounallah, "Robust min-norm algorithms for coherent sources doa estimation based on toeplitz matrix reconstruction methods," *International Journal of Wireless and Mobile Computing*, vol. 24, no. 1, pp. 9–16, 2023.

[12] J.-P. Lachaux, A. Lutz, D. Rudrauf, D. Cosmelli, M. Le Van Quyen, J. Martinerie, and F. Varela, "Estimating the time-course of coherence between single-trial brain signals: an introduction to wavelet coherence," *Neurophysiologie Clinique/Clinical Neurophysiology*, vol. 32, no. 3, pp. 157–174, 2002.

[13] M. Rhudy, B. Bucci, J. Vipperman, J. Allanach, and B. Abraham, "Microphone array analysis methods using cross-correlations," in *ASME International Mechanical Engineering Congress and Exposition*, vol. 43888, pp. 281–288, 2009.

[14] W. Suleiman, P. Parvazi, M. Pesavento, and A. M. Zoubir, "Non-coherent direction-of-arrival estimation using partly calibrated arrays," *IEEE Transactions on Signal Processing*, vol. 66, no. 21, pp. 5776–5788, 2018.

[15] Y. Liao, A. Abouzaid, and R. April, "Resolution improvement for music and root music algorithms.," *J. Inf. Hiding Multim. Signal Process.*, vol. 6, no. 2, pp. 189–197, 2015.

[16] A. Naceur, "Improved polynomial rooting of capon's algorithm to estimate the direction-of-arrival in smart array antenna," *Journal of Microwaves, Optoelectronics and Electromagnetic Applications*, vol. 17, no. 4, pp. 494–508, 2018.

[17] N. Aounallah, "Performance enhancement of capon's doa algorithm using covariance matrix decomposition," *Engineering Proceedings*, vol. 14, no. 1, p. 7, 2022.

[18] A. Naceur, "Improving the resolution performance of min-norm and root-min-norm algorithms for adaptive array antenna," in *2017 5th International Conference on Electrical Engineering-Boumerdes (ICEE-B)*, pp. 1–5, IEEE, 2017.

[19] F. Hijlkema, "Direction-of-arrival estimation using a machine learning framework," Master's thesis, University of Twente, 2022.

[20] M. A. Al-Sadoon, *Direction Finding and Beamforming Techniques using Antenna Array for Wireless System Applications*. PhD thesis, University of Bradford, 2019.

[21] A. Naceur and L. Smail, "Improved doa estimation algorithms using modified covariance matrix," in *2022 19th International Multi-Conference on Systems, Signals & Devices (SSD)*, pp. 1737–1742, IEEE, 2022.

[22] Y. Hou, X. Wang, L. Ding, X. Jin, and Q. Zhang, "Doa-estimation method based on improved spatial-smoothing technique," *Mathematics*, vol. 12, no. 1, p. 45, 2023.